Roma - 17/05/2024

Doping and Hyper-doping

Enrico Di Russo

OUTLINE

- **PART I: Heavy doping effects in GaN and $Al_xGa_{1-x}N$**
  - *i)* Mg doping (p-type)
  - *ii)* Ge doping (n-type)
  - *iii)* Tunnel junction

- **PART II: Hyper-doping in Ge and Si by pulsed laser melting**
  - *i)* B and Ga doping (p-type)
  - *ii)* Sb doping (n-type)

Part I

Heavy doping effects in GaN

Mg doping

Doping in GaN

❖ **p-type** doping is still imperfect; magnesium (**Mg**) is the only impurity that can produce p-type GaN, and it suffers from significant limitations.

❖ **n-type** doping is straightforward, and can be achieved by adding elements such as silicon (**Si**) or germanium (**Ge**).

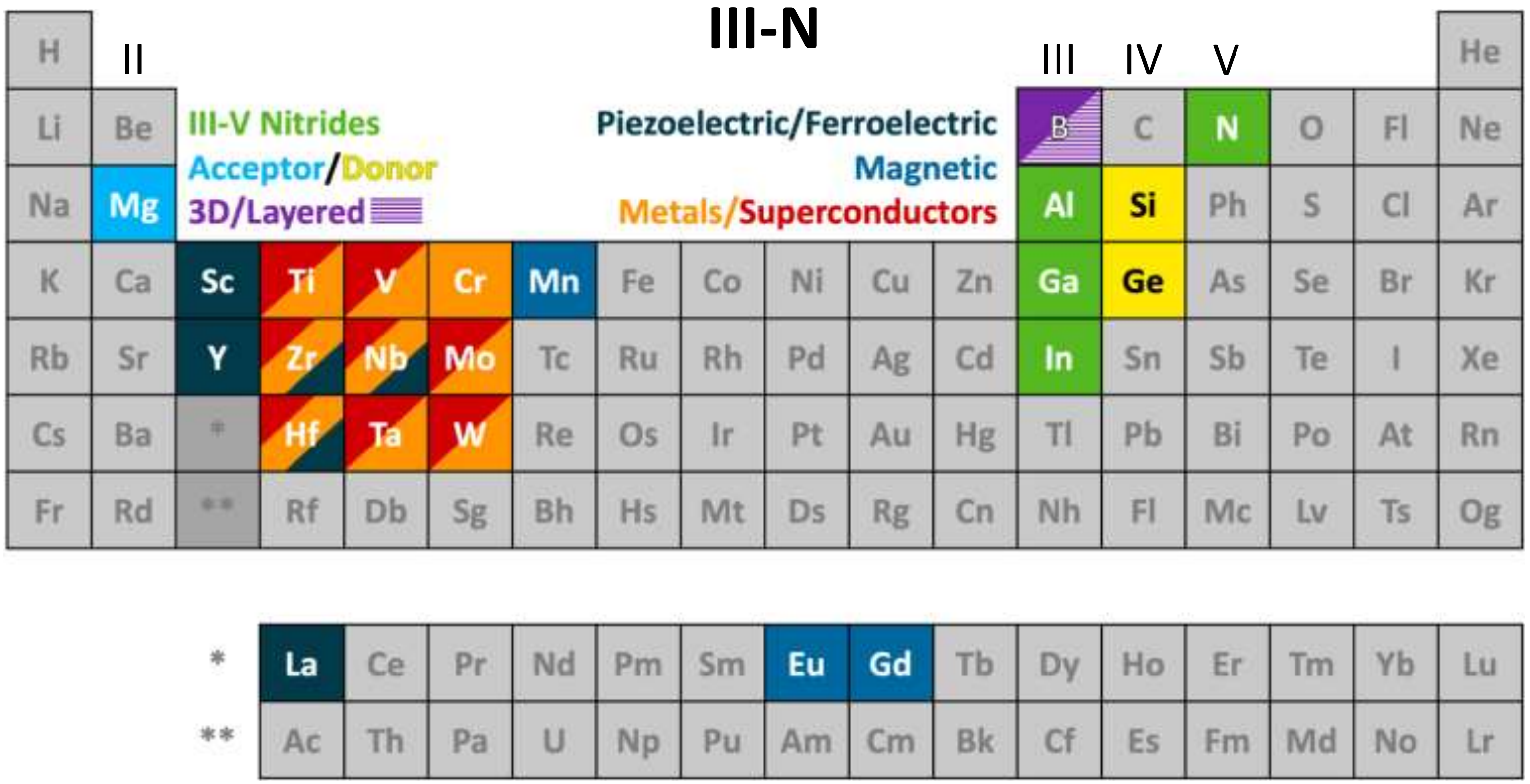

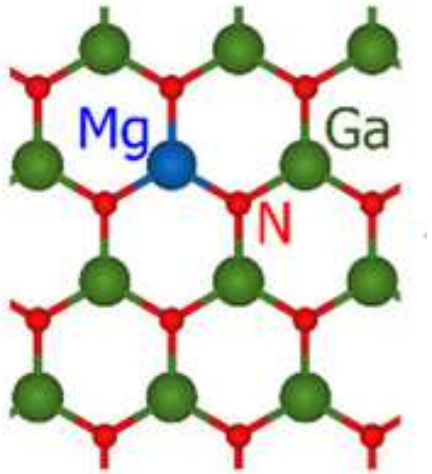

- **Substitutional doping:** atoms of the host metal (Ga) are replaced by foreign atoms (Mg, Si, Ge).

Doping in GaN

- The **ionization energy of a dopant** determines the fraction of dopants that contributes free carriers at a given temperature.

intrinsic | **n-type** | **p-type**

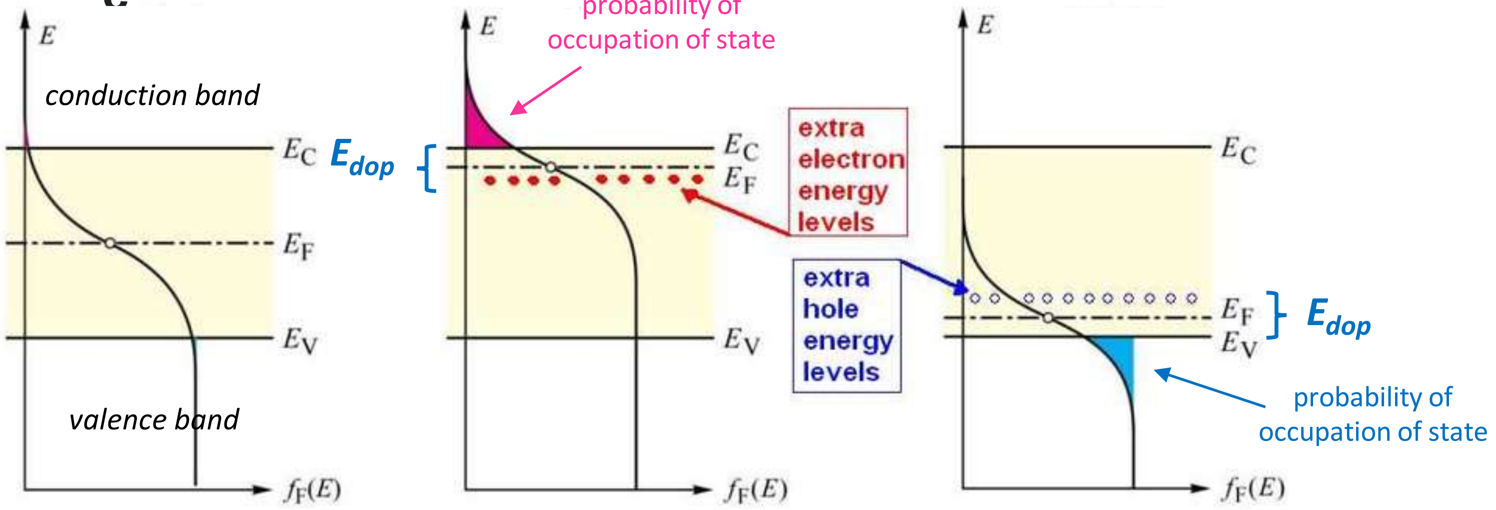

$$f(E) = \frac{1}{e^{(E-E_F)/kT}+1}$$

Si/Ge-doping

Mg-doping

Ionization energies (E_{dop}) in wurtzite GaN [1]

GaN		Theoretical values (meV)
Donors	V_N	30
	Si	30
	O	30
Acceptors	V_{Ga}	158
	Mg	158
	Be	158

Donors: *Full ionization*

Acceptors: *Partial ionization*

At room temperature: **kT = 25 meV**

[1] S. Lin et al., Journal of Materials Science 47 (2012): 4595-4603. *doi.org/10.1007/s10853-012-6321-6*

Mg-doping in GaN

Mg is the most common used **acceptor** (p-doping) in GaN

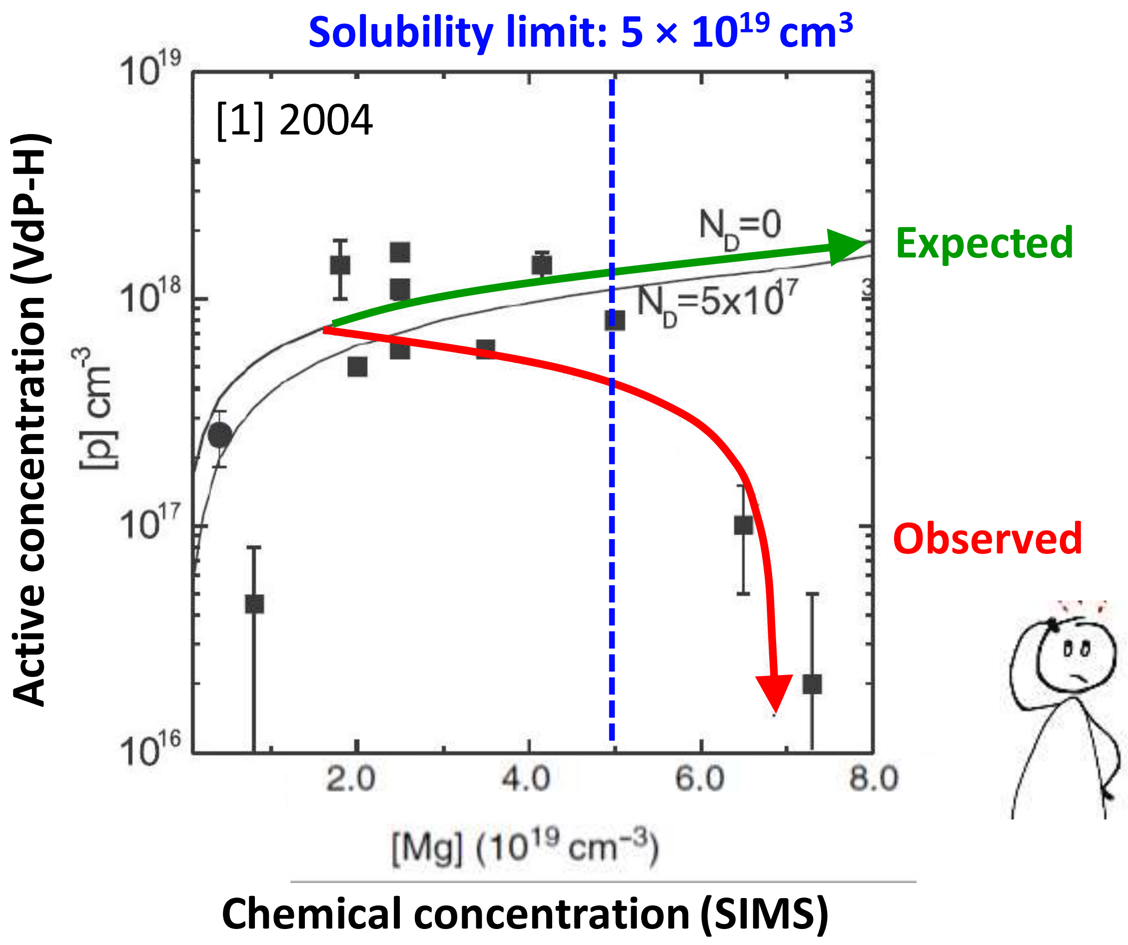

- Since the activation energy of Mg doping is quite high at room temperature (≈ 150 meV), only a small fraction of substitutional Mg atoms is typically ionized (≈ 2 %) [2]
- Mg is <u>only in part</u> incorporated in electrically active sites of GaN.

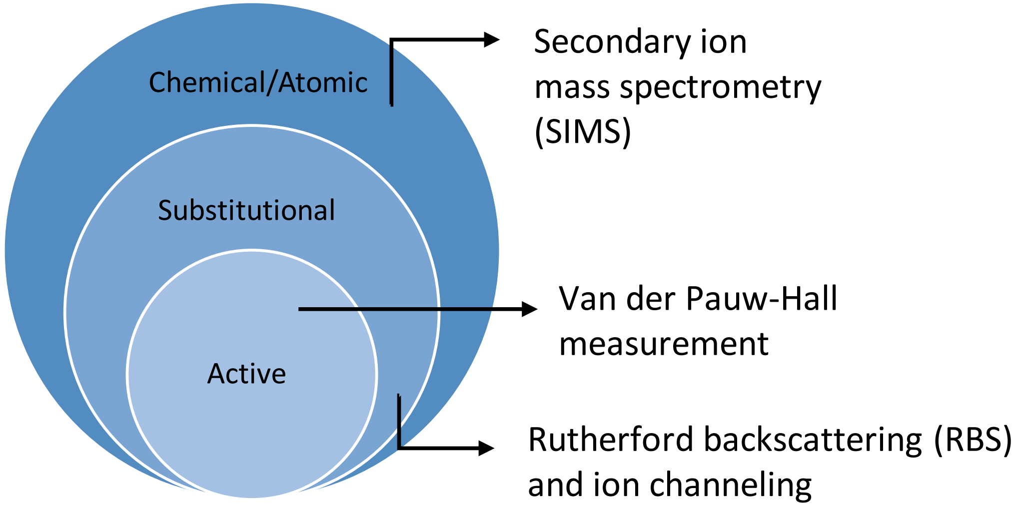

[1] Leroux et al., The European Physical Journal Applied Physics 27.1-3 (2004): 259-262. *doi.org/10.1051/epjap:2004119-2*
[2] Nakamura et al., Japanese Journal of Applied Physics 31.5R (1992): 1258. *doi.org/*10.1143/JJAP.31.1258

Pyramidal inversion domains (PIDs)

SIMS Mg concentration: 6.7 × 10^{19} cm^3

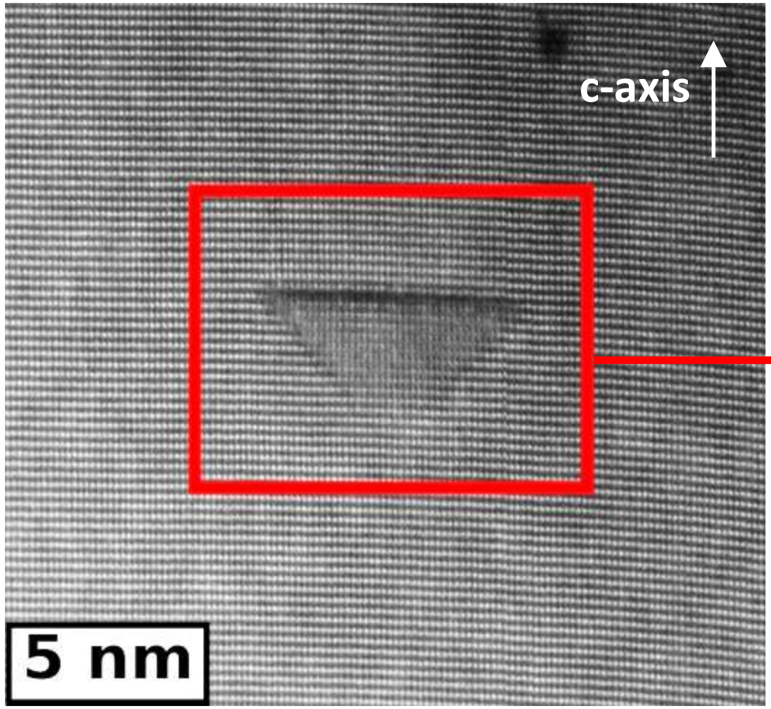

[1]

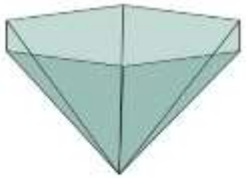

GaN unit cell

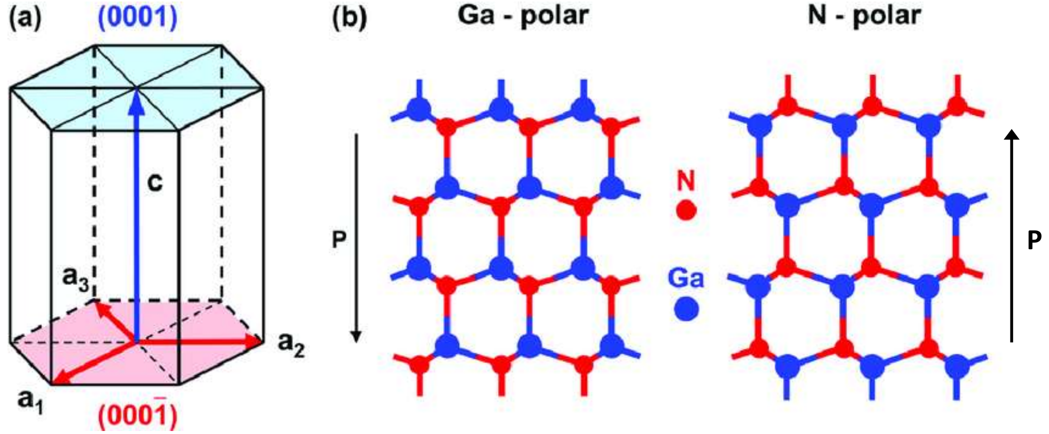

- ❖ High levels of Mg-doping strongly influence the **microstructure of GaN**

- High Mg-concentrations lead to the formation of **PYRAMIDAL INVERSION DOMAINS (PIDs)** that combine structural displacements with compositional replacements effects.

- PIDs present a 2–6 nm width hexagonal base in the {0001} plane and six {1213} side facets, exhibiting also an **inversion of the GaN polarity** compared to the matrix.

- In the early 2000s, the detailed atomic structure of PIDs was still controversial.

[1] Persson et al., Scientific Reports 12.1 (2022): 17987. doi.org/10.1038/s41598-022-22622-1

Transmission Electron Microscopy (TEM)

❖ Analytical TEM is the key technique for the investigation **of local composition** in crystals

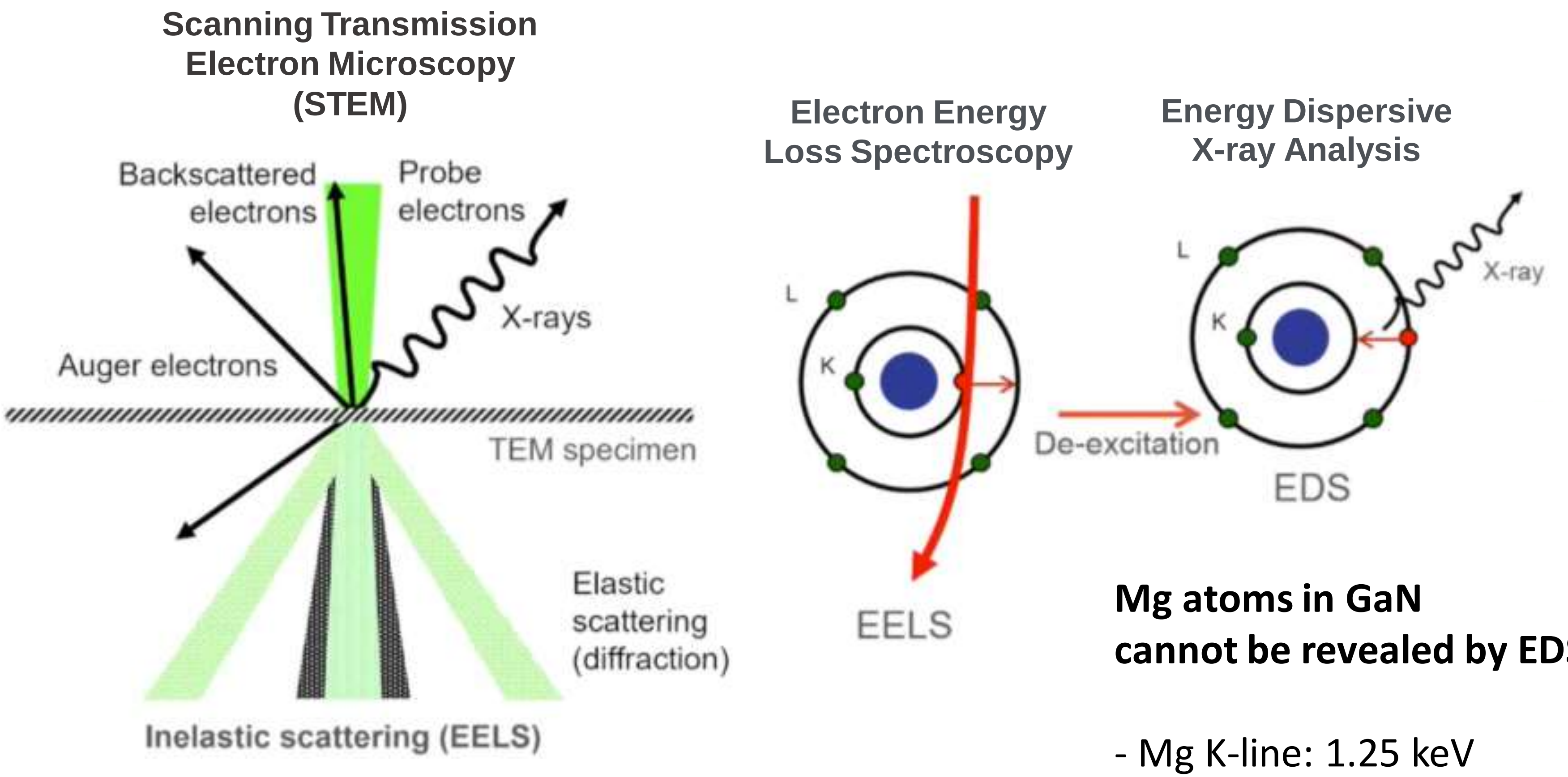

Mg atoms in GaN cannot be revealed by EDS

- Mg K-line: 1.25 keV
- Ga L-line: 1.19 keV

Mg segregation effects in PIDs

HR-STEM

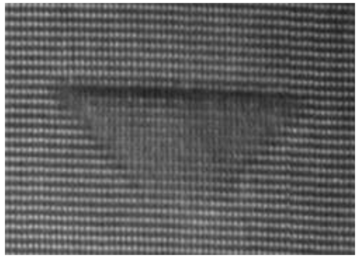

EELS

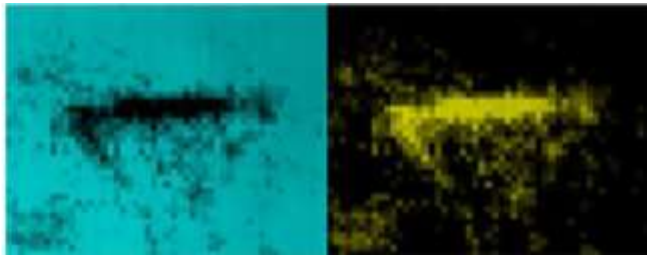

[2]

Ga atoms   Mg dopants

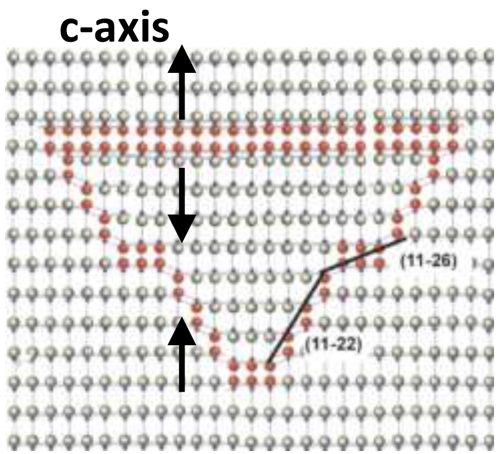

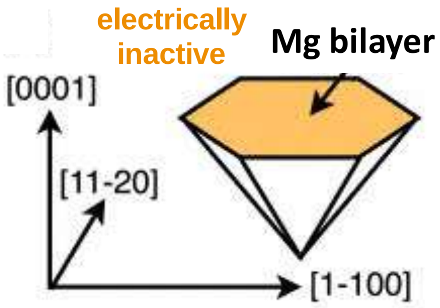

- EELS observations in CNRS-CRHEA (2000): the inversion domain boundaries are formed by **Mg_3N_2** layers [1].
- HAADF-STEM and EELS observations of PIDs {0001} facet have recently shown the presence of a pure Mg layer inserted between two N layers that delimit the inner and the outer of a PIDs base [2].

Because all these Mg atoms are electrical inactive, a strong reduction in free-hole concentration in highly Mg-doped GaN occurs [2,3].

QUANTIFICATION ISSUES:

Quantitative chemical mapping of compounds with solute atom concentrations of less than 1 at.% are difficult if at all possible.

[1] Vennéguès et al., Applied Physics Letters 77.6 (2000): 880-882. *doi.org/10.1063/1.1306421*
[2] Persson et al., Scientific Reports 12.1 (2022): 17987. *doi.org/10.1038/s41598-022-22622-1*
[3] Leroux et al., The European Physical Journal Applied Physics 27.1-3 (2004): 259-262. *doi.org/10.1051/epjap:2004119-2*

Atom probe tomography (APT)

$$\frac{m}{n} = 2eV_{DC}\frac{t^2}{L^2}$$

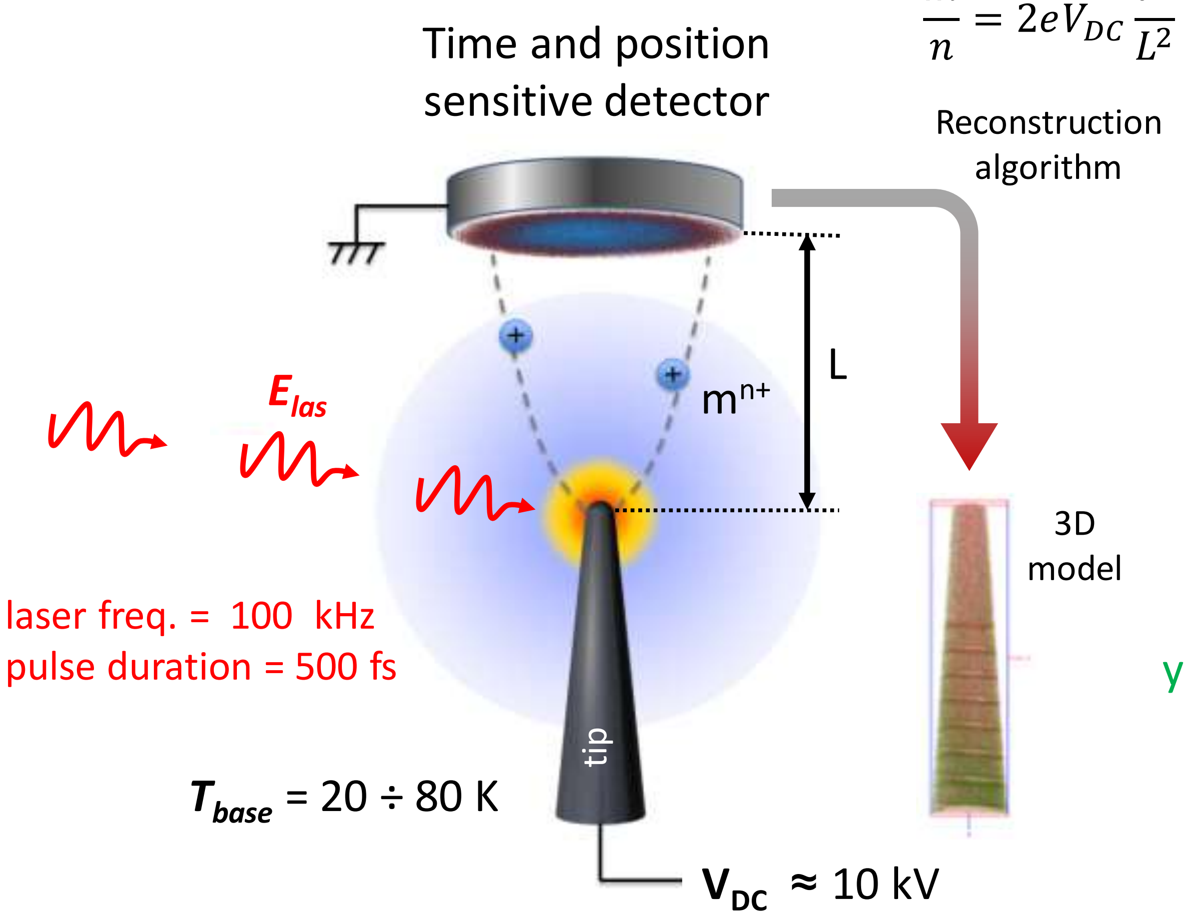

- (About) same chemical sensitivity for all elements.
- Spatial resolution ~2 nm, detection limit ~10^{19} cm^3.
- Detection efficiency of about 20-60 %.

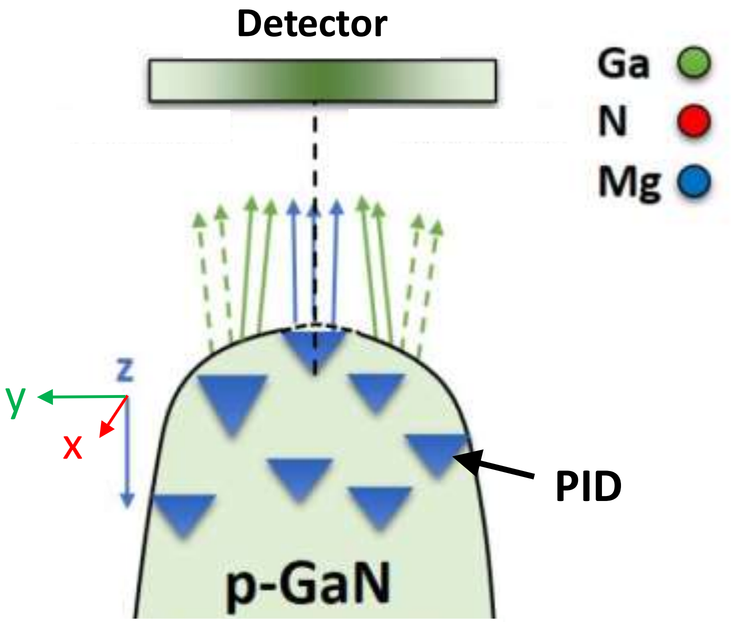

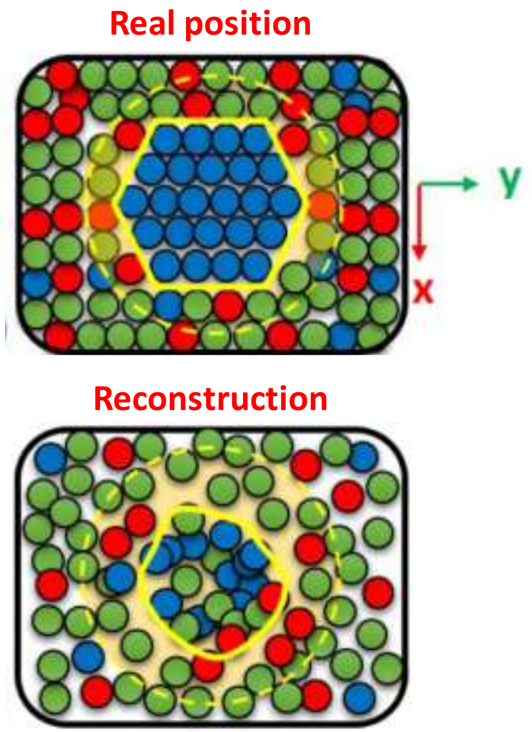

Mg segregation effects in PIDs

Growth temperature: 900°C → 1010°C → 1030°C

Mg concentration:
5×10^{19} cm³

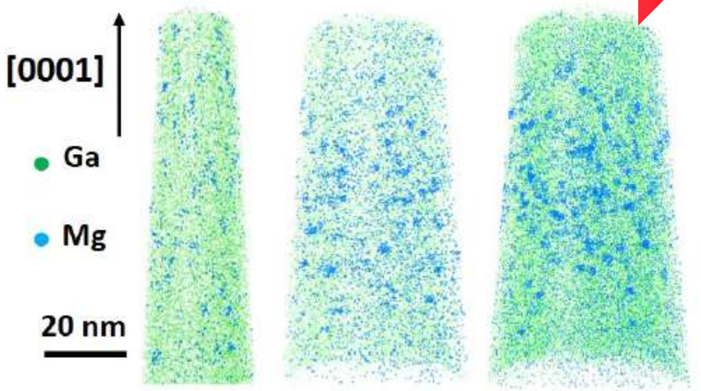

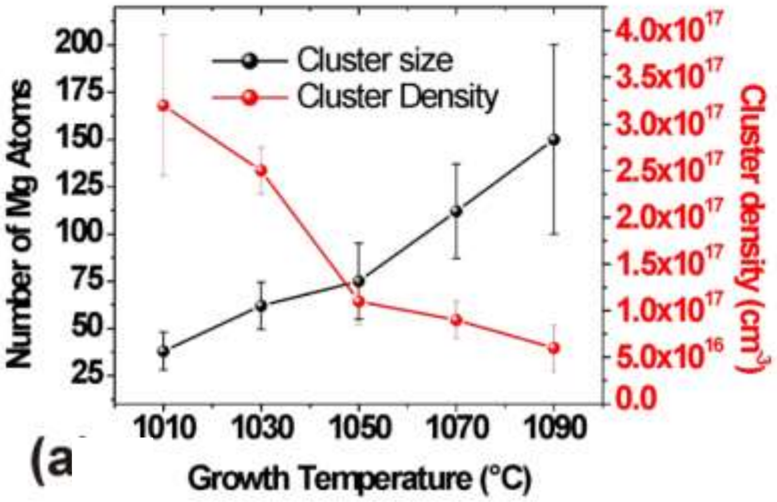

The "cluster" **size** increases

Mg concentration: 1×10^{19} cm³ → 7×10^{19} cm³ → 7×10^{19} cm³

Growth temperature:
950 °C

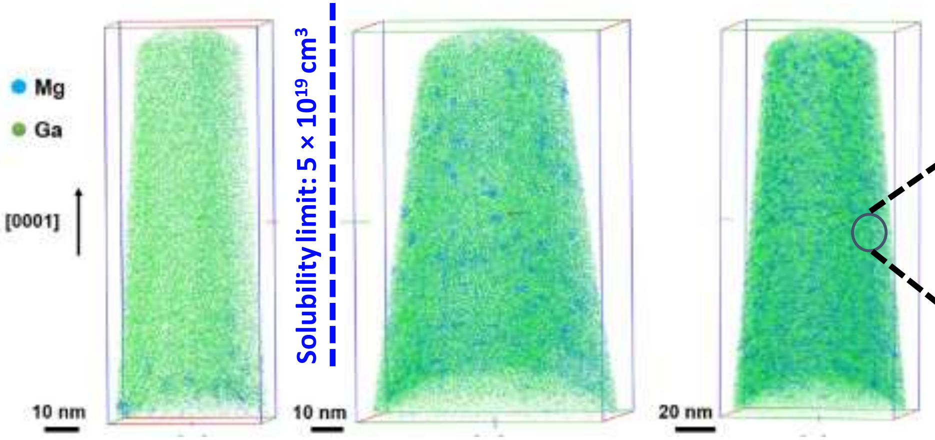

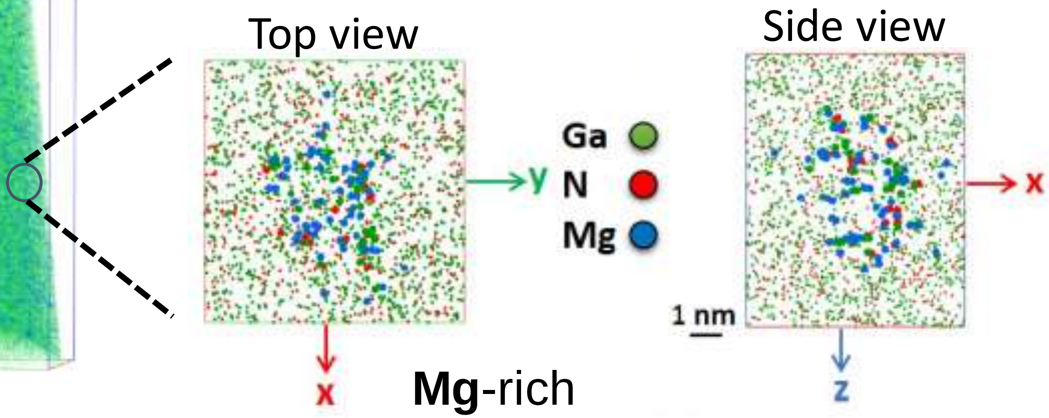

Mg-rich
"clusters"

The "cluster" **number** increases

[1] L. Amichi, Ph.D thesis. CEA-LETI, Université de Grenoble-Alpes, Grenoble (France).
[2] L. Amichi et al., Nanotechnology 31.4 (2019): 045702. *doi.org/ 10.1088/1361-6528/ab4a46*

Transmission Electron Microscopy (TEM): electron holography

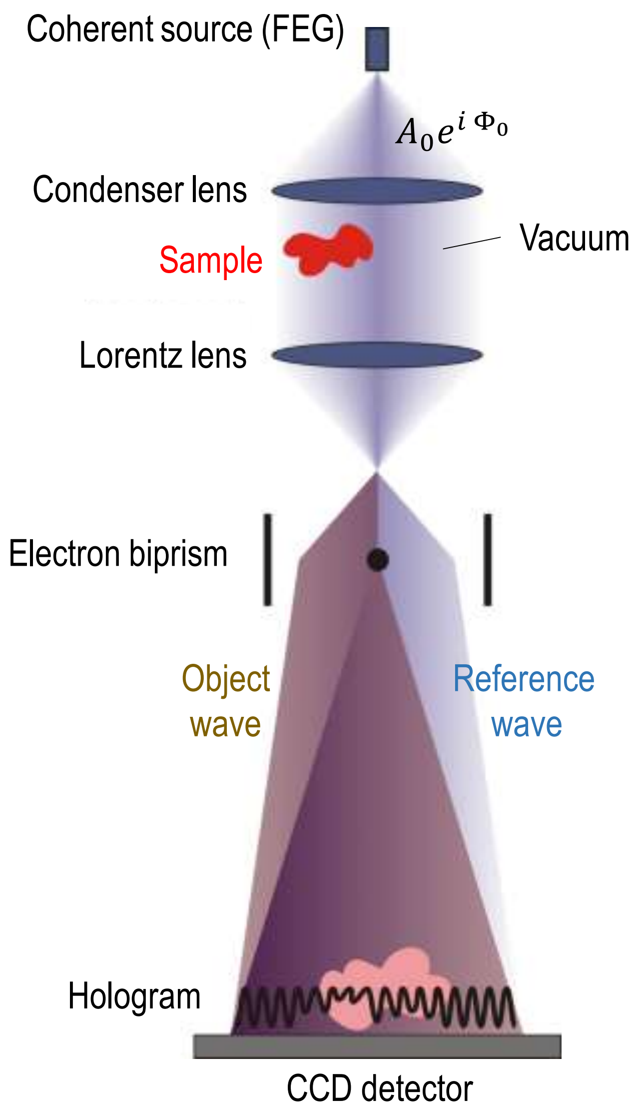

- High spatial and temporal coherence of the electron beam required.

Hologram

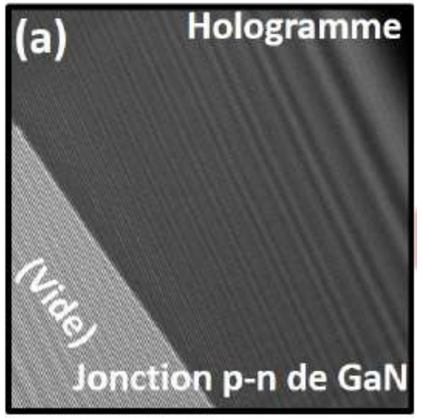

object image + interference pattern

Reconstruction algorithm

Phase

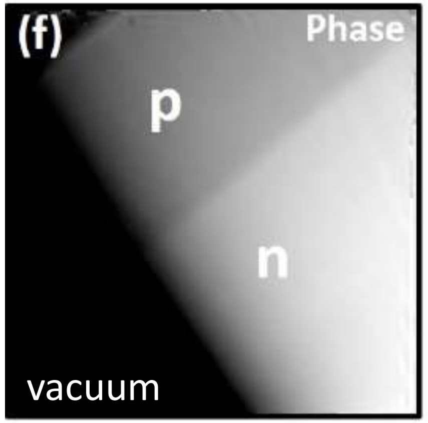

[1]

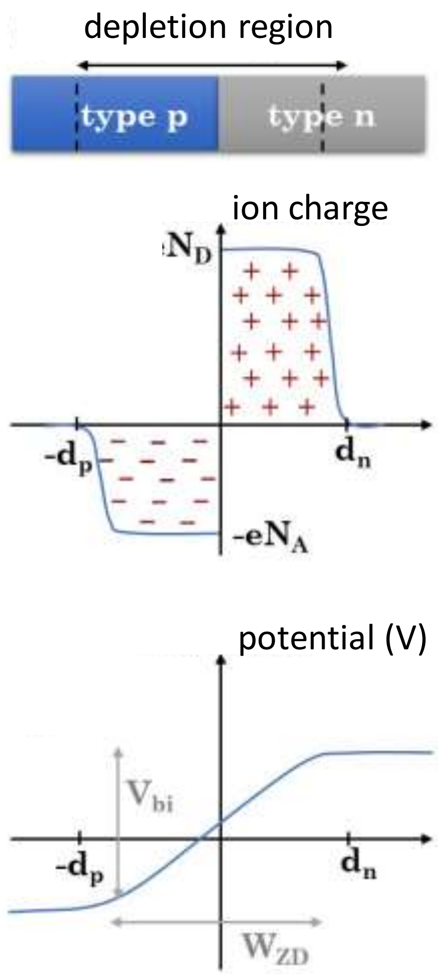

$$\phi_e = \phi_{dopant} + \phi_{MIP} = C_E \int_0^t V_{dopant}(r,z)dz + C_E \int_0^t V_0(r,z)d(z)$$

[1] L. Amichi, Ph.D thesis. CEA-LETI, Université de Grenoble-Alpes, Grenoble (France).

Mg activation

Electron holography

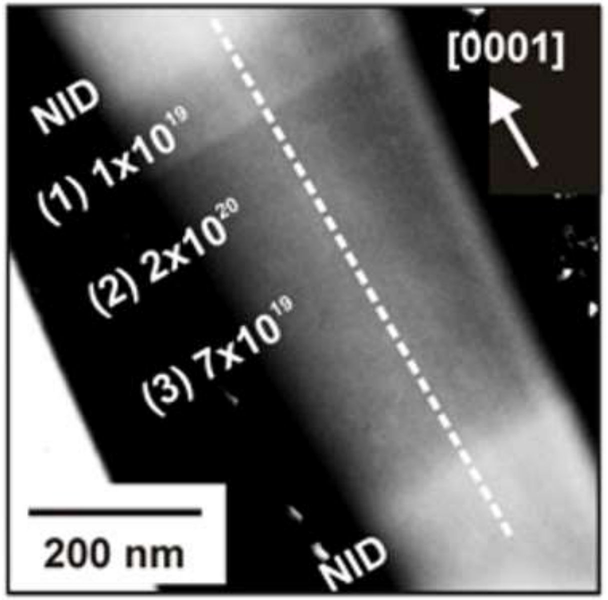

Grown temperature: 950 °C

$$\phi_{dopant} = C_E \int_0^t V_{dopant}(r, z)dz$$

Nextnano simulations

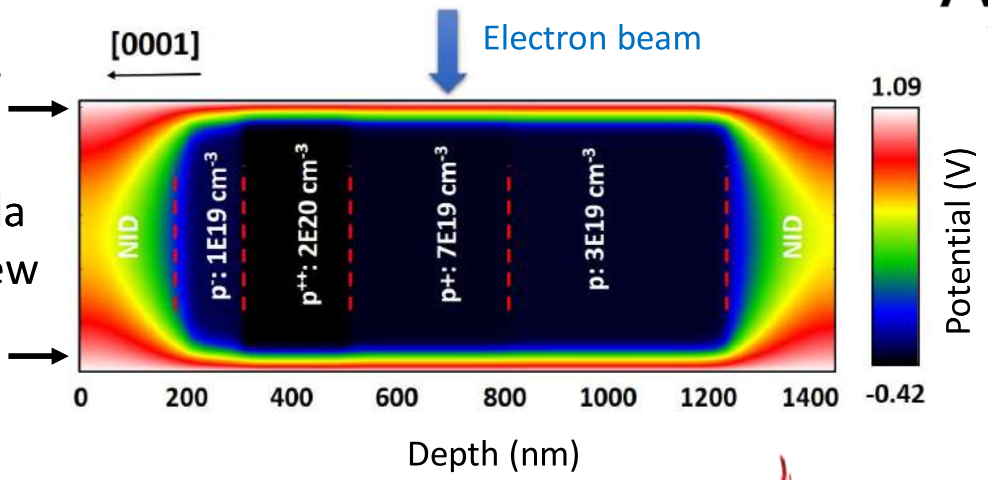

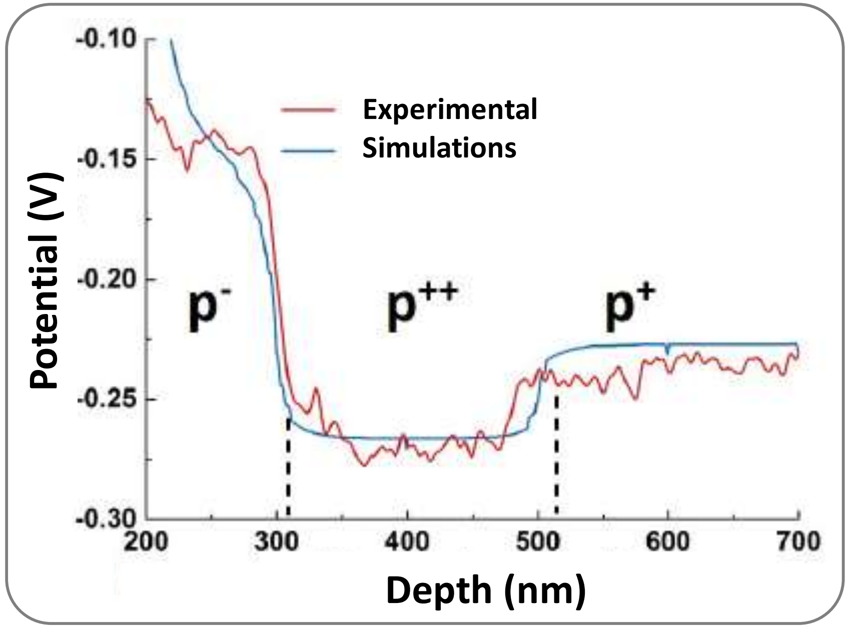

- The phase shift measured is correlated with the local potential. This last depends only on the **active doping**.
- Numerical calculations allows to assess the active doping concentration at the nanometric scale.

[1] L. Amichi et al., Journal of Applied Physics, 2020, 127 (6), 065702. *doi.org/10.1063/1.5125188*

Mg activation

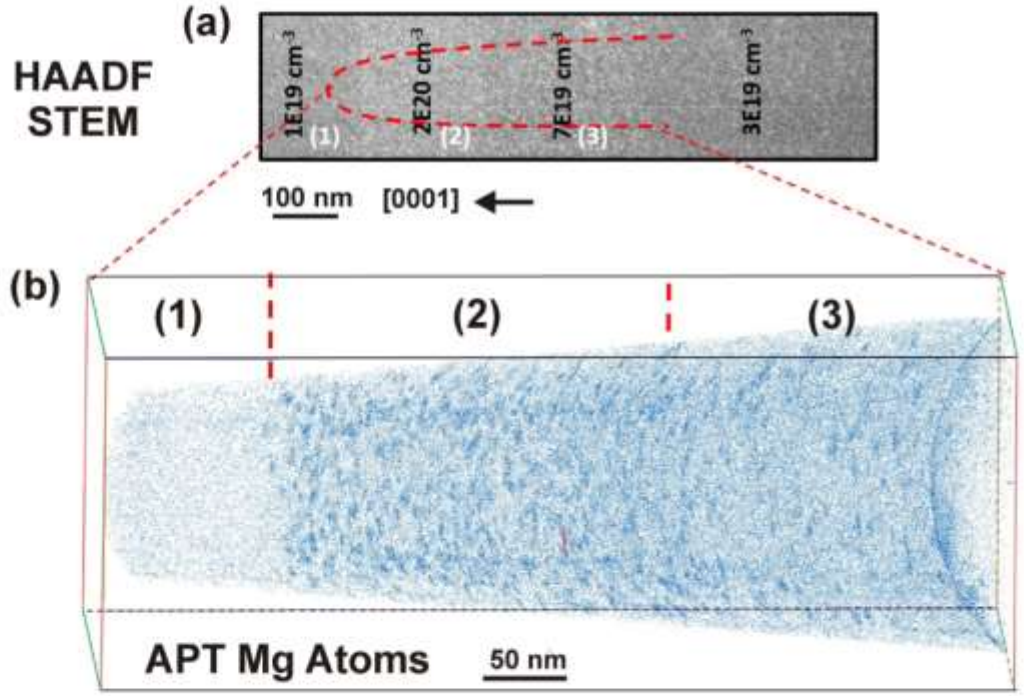

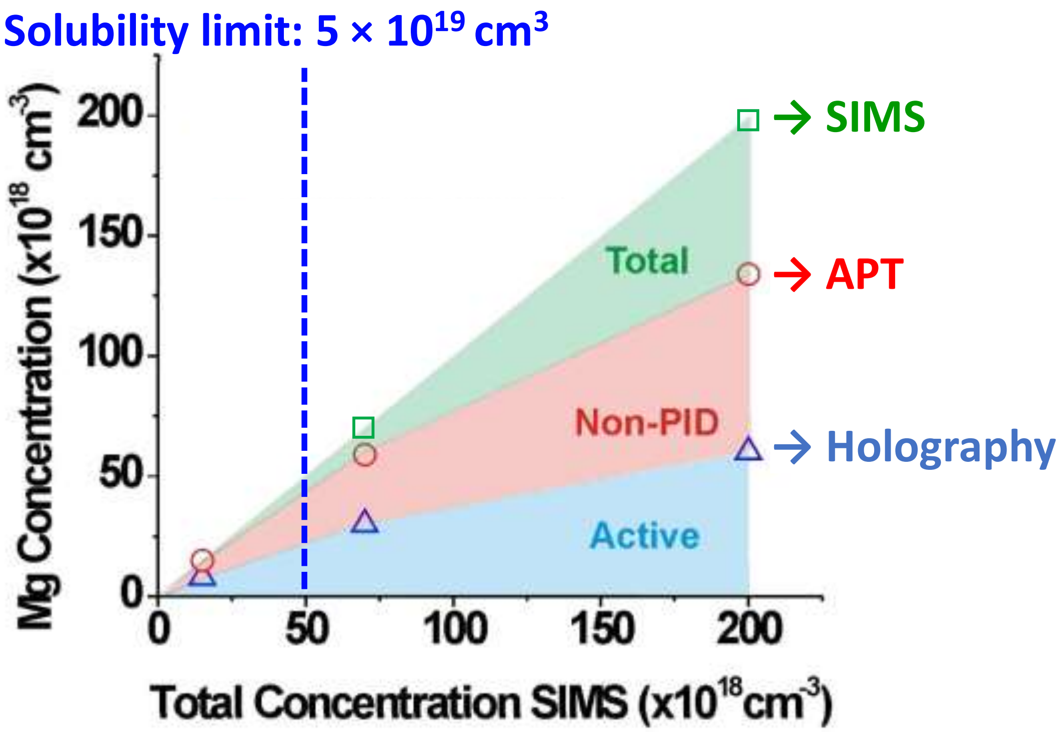

- APT reveals that only a fraction of the total Mg atoms is not segregated within the PIDs.
- Electron holography clearly indicates that only a part of Mg atoms in the matrix is active, due to the **large activation energy of Mg in GaN (~200 meV)**.

[1] L. Amichi et al., Journal of Applied Physics, 2020, 127 (6), 065702. *doi.org/10.1063/1.5125188*

Part I

Heavy doping effects in $Al_xGa_{1-x}N$

Ge doping

Si- and Ge-doping

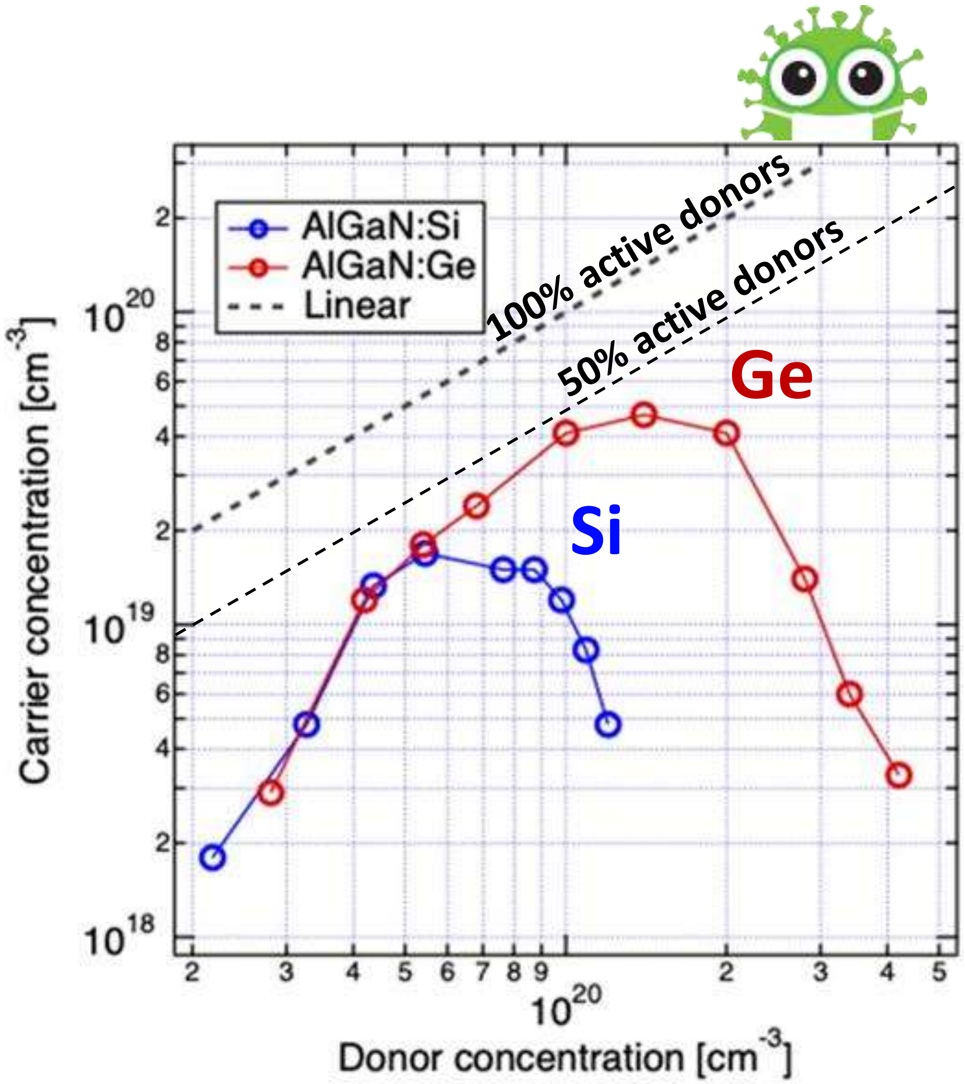

Why Ge-doping in $Al_xGa_{1-x}N$?

Attaining **low resistivity $Al_xGa_{1-x}N$** is the keystone to improve the efficiency of light emitting devices in the UV spectral range.

- Ge, like Si, is a shallow donor in GaN, with a theoretical activation energy of 30 meV.

- **The ionic radius of a Ge atom is similar to that of Ga**.

- The metal-nitrogen bond length changes by only 1.4% with Ge, compared to 5.5% with Si. Hence Ge can occupy the Ga lattice site causing far less lattice distortion than other dopants like Si and O.

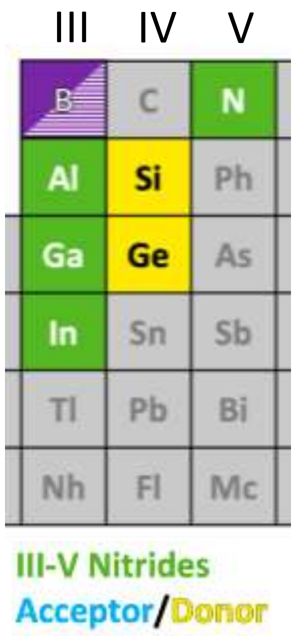

S. Washiyama et al., Appl. Phys. Lett. 118, 042102 (2021). *doi.org/10.1063/5.0035957*

Ge-doping in $Al_xGa_{1-x}N$ – low Al atomic fraction

$Al_{0.2}Ga_{0.8}N$
$[Ge] = 2.3 \times 10^{20}\ cm^{-3}$

Ga Al Ge

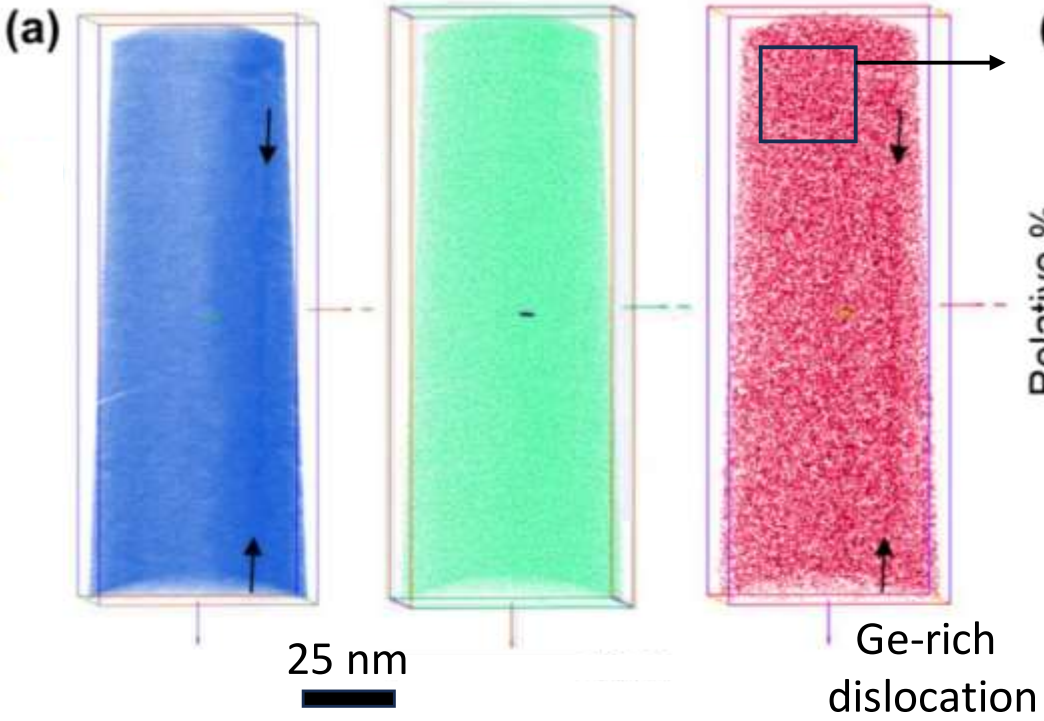

Clustering statistical test:

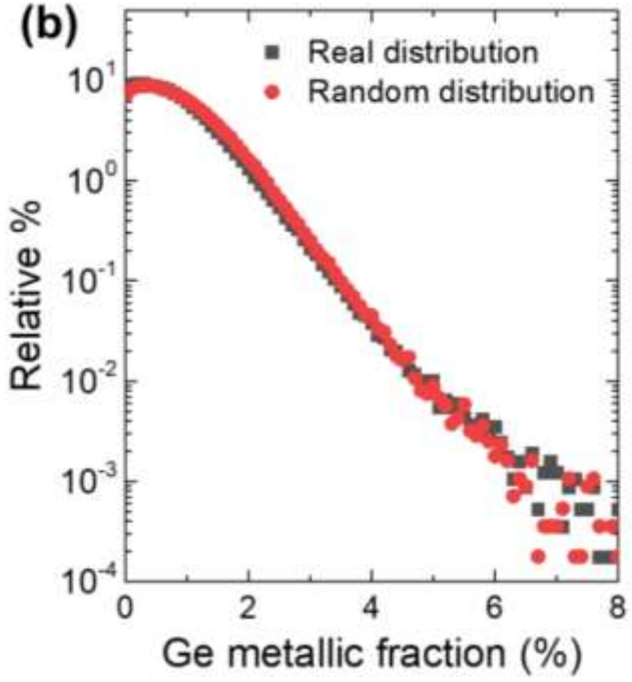

$$y_{Ge} = \frac{Ge}{Ga + Al + Ge}$$

- Some **threading dislocations** are decorated with Ge.
- **No clustering** at the nanometer scale in the $Al_{0.2}Ga_{0.8}N$ matrix. Ge atoms are randomly distributed.

Note: The presence of clusters at the level of 2−5 atoms would be below the detection limit of APT.

C. Bougerol et al., ACS Appl. Mater. Interfaces 2021, 13, 3, 4165–4173. *doi.org/10.1021/acsami.0c19174*

Ge-doping in $Al_xGa_{1-x}N$ – medium Al atomic fraction

$Al_{0.45}Ga_{0.55}N$
$[Ge] = 2.5 \times 10^{20}\ cm^{-3}$

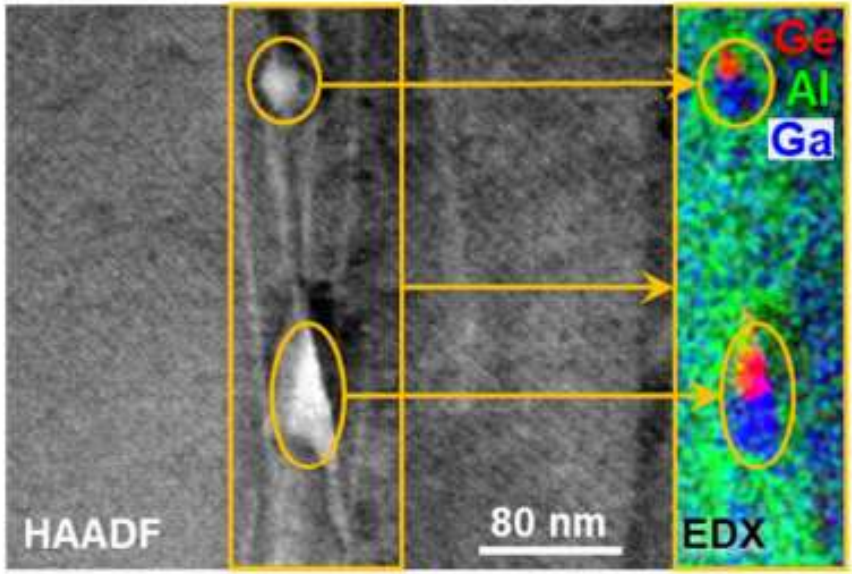

- Marked **inhomogeneity in the Ge distribution** associated with a nonuniform distribution of Al and Ga: nanometer-size Ge-rich regions are located on top of Ga-rich areas along the growth direction.

$Al_{0.57}Ga_{0.43}N$
$[Ge] = 2.0 \times 10^{20}\ cm^{-3}$

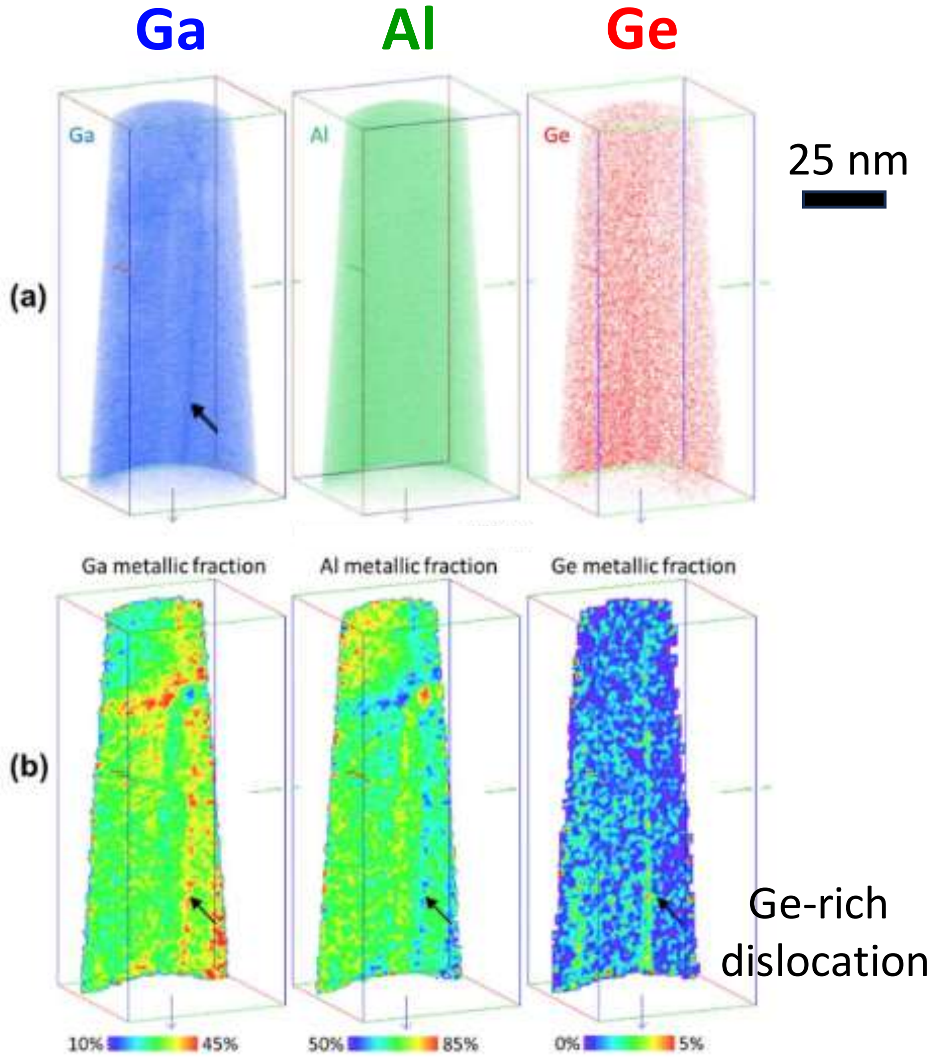

C. Bougerol et al., ACS Appl. Mater. Interfaces 2021, 13, 3, 4165–4173. *doi.org/10.1021/acsami.0c19174*

Ge-doping in $Al_xGa_{1-x}N$ – high Al atomic fraction

AlN

[Ge] = 2.0 ×10^{20} cm^{-3}

SEM-EDS

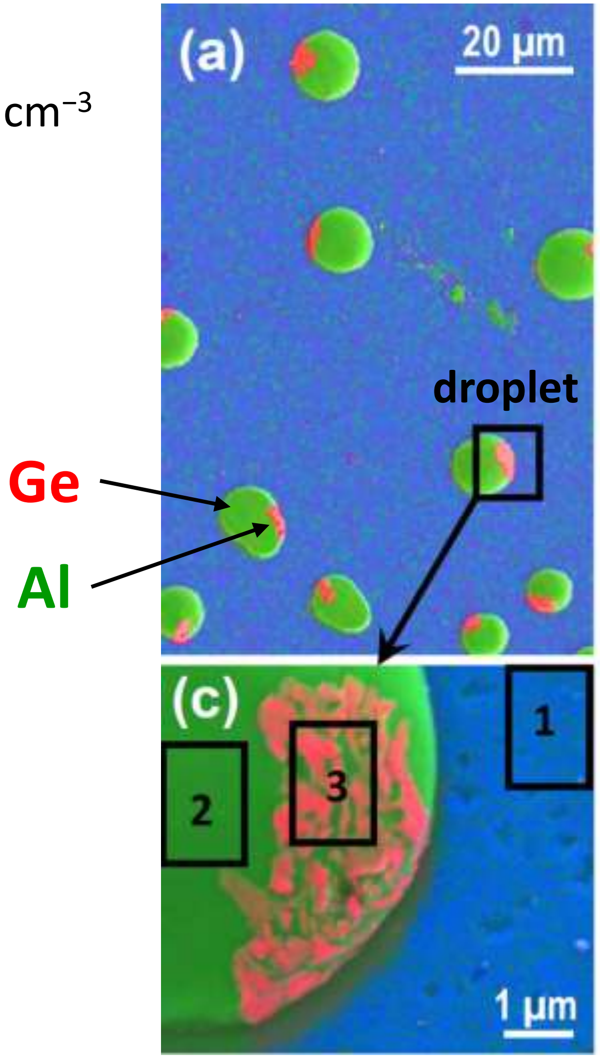

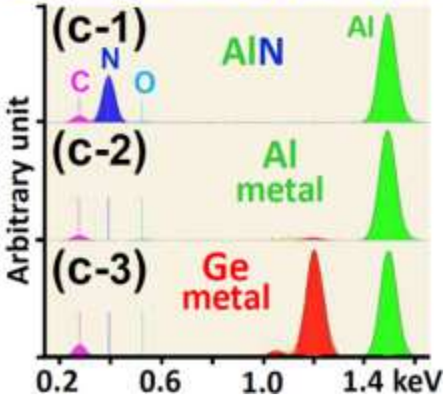

- Presence of **metallic Ge** at the surface in highly doped $Al_xGa_{1-x}N$ ($x \geq 0.4$) samples.
- Metallic Ge appears systematically located at the periphery of the surface droplets.

C. Bougerol et al., ACS Appl. Mater. Interfaces 2021, 13, 3, 4165–4173. *doi.org/10.1021/acsami.0c19174*

Ge-doping in $Al_xGa_{1-x}N$

Ga atoms density in GaN: 4.5×10^{22}

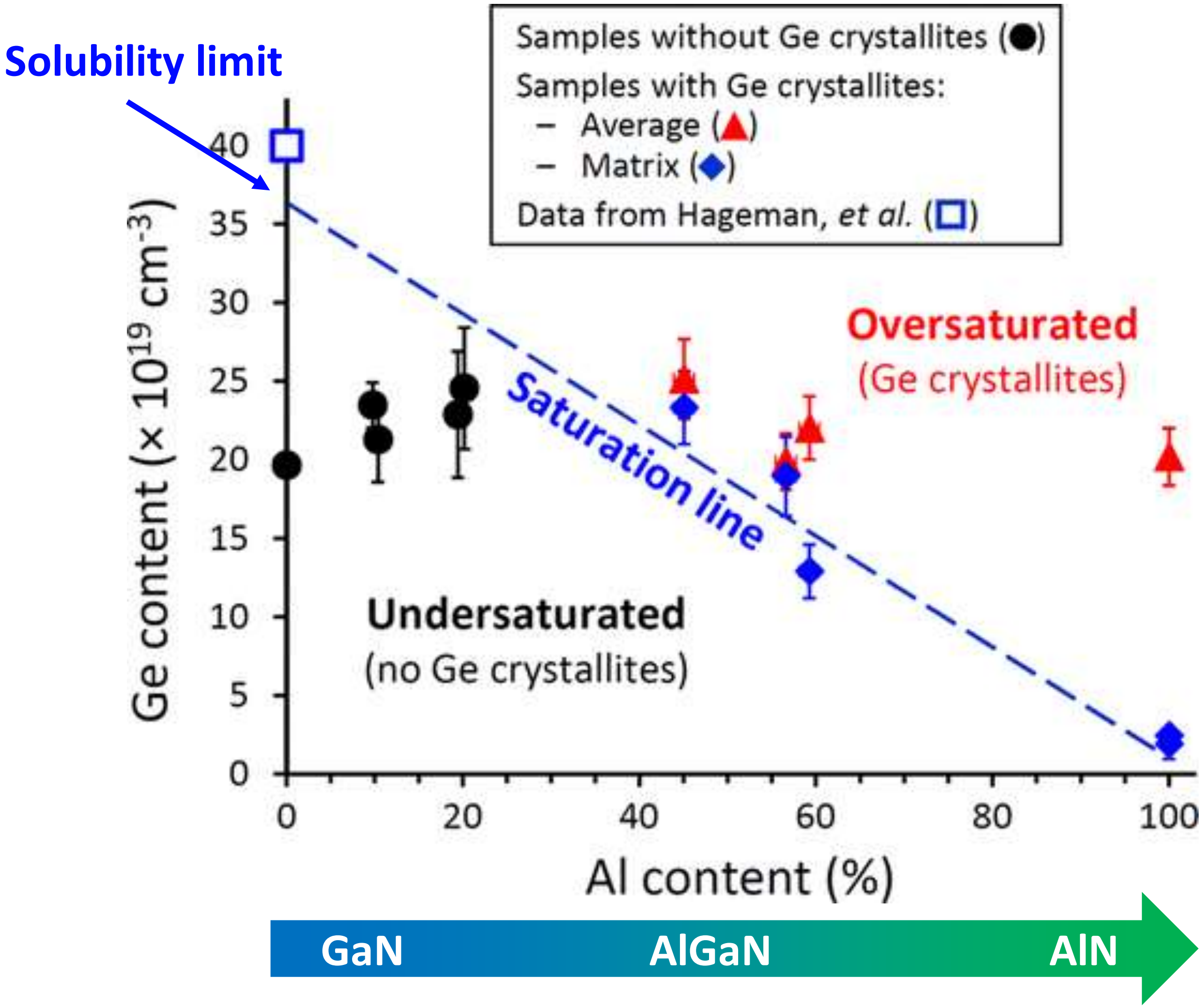

Issue of Ge solubility in $Al_xGa_{1-x}N$:

- ❖ Diffusion of Ge along structural defects.
- ❖ Formation of Ge precipitates.
- ❖ Formation of Ge surface crystallites.

Conclusions:

- The incorporation of Ge in AlN is at least one order of magnitude lower than in GaN.
- The saturation threshold increases linearly with the Ga mole fraction of the ternary alloy, which would suggest that the incorporation of Ge in AlGaN takes place by substitution of Ga atoms.
- **With this assumption, the maximum percentage of Ga sites occupied by Ge would saturate around 1%.**

C. Bougerol et al., ACS Appl. Mater. Interfaces 2021, 13, 3, 4165–4173. *doi.org/10.1021/acsami.0c19174*

Part I

Heavy doping effects in GaN

Tunnel junction

Ge/Mg hybrid-tunnel junction

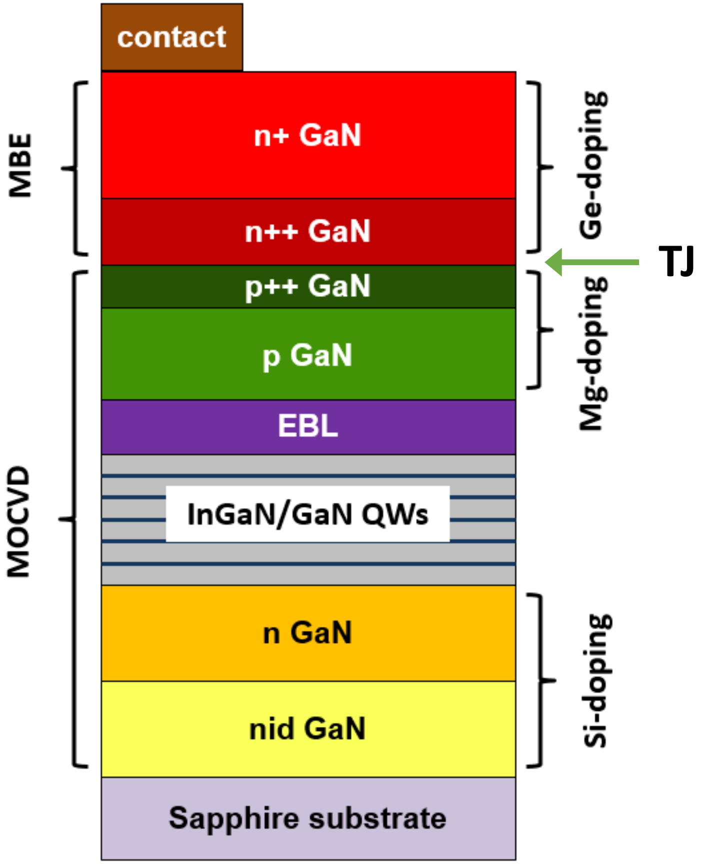

- **TJ improves hole injection into the p-doped GaN**.
- Depletion region width: $w_d \approx \sqrt{\frac{2\varepsilon V_{bi}(N_A + N_D)}{e N_A N_D}}$
- Quantum tunnelling probability: $T_i \approx e^{-\frac{4}{3} w_d \sqrt{\frac{2m^* V_{bi}}{\hbar}}}$

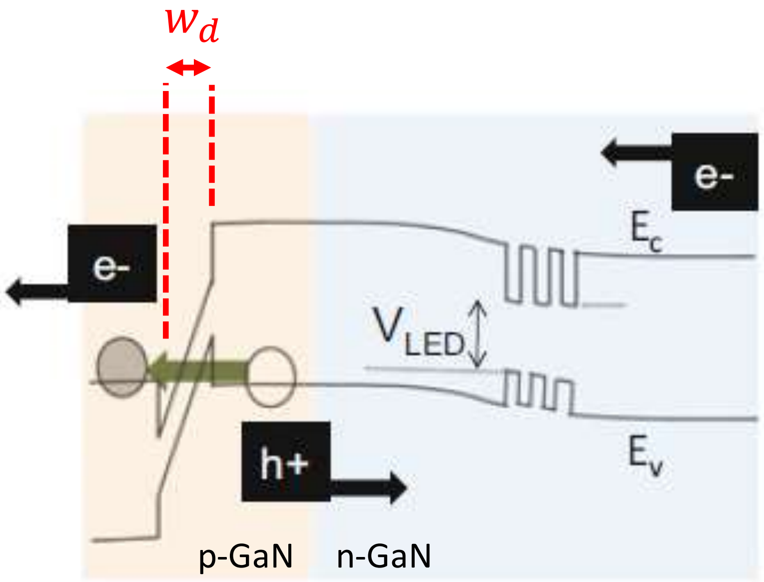

Reverse bias

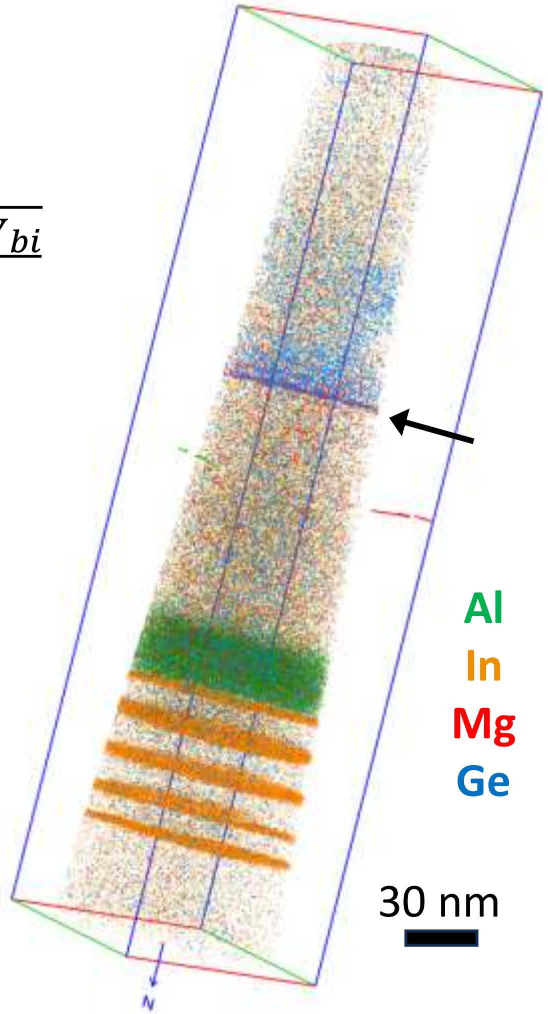

E. Di Russo, et al., Nanotechnology 31.46 (2020): 465706. *doi.org/10.1088/1361-6528/ab996c*

Ge/Mg hybrid-tunnel junction

$$\varphi(x,y) = C_E \int_0^t V_E(x,y,z)dz$$

where: $V_E(x,y,z) = V_{MIP} + V_{dopant}$

HAADF-STEM

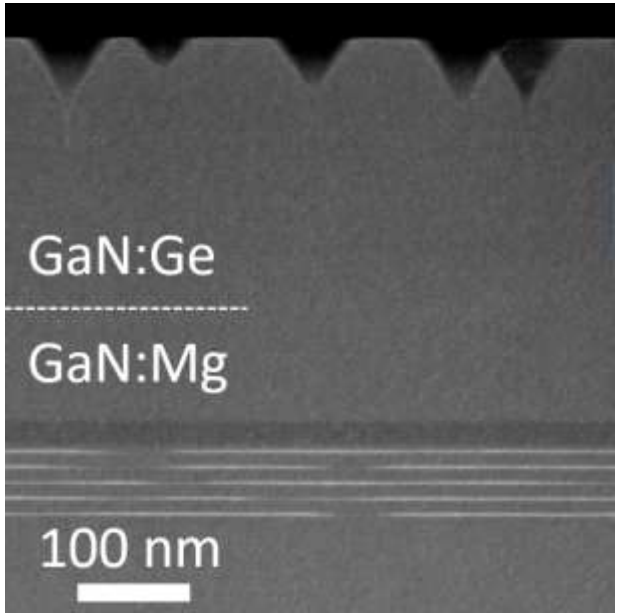

Electron holography

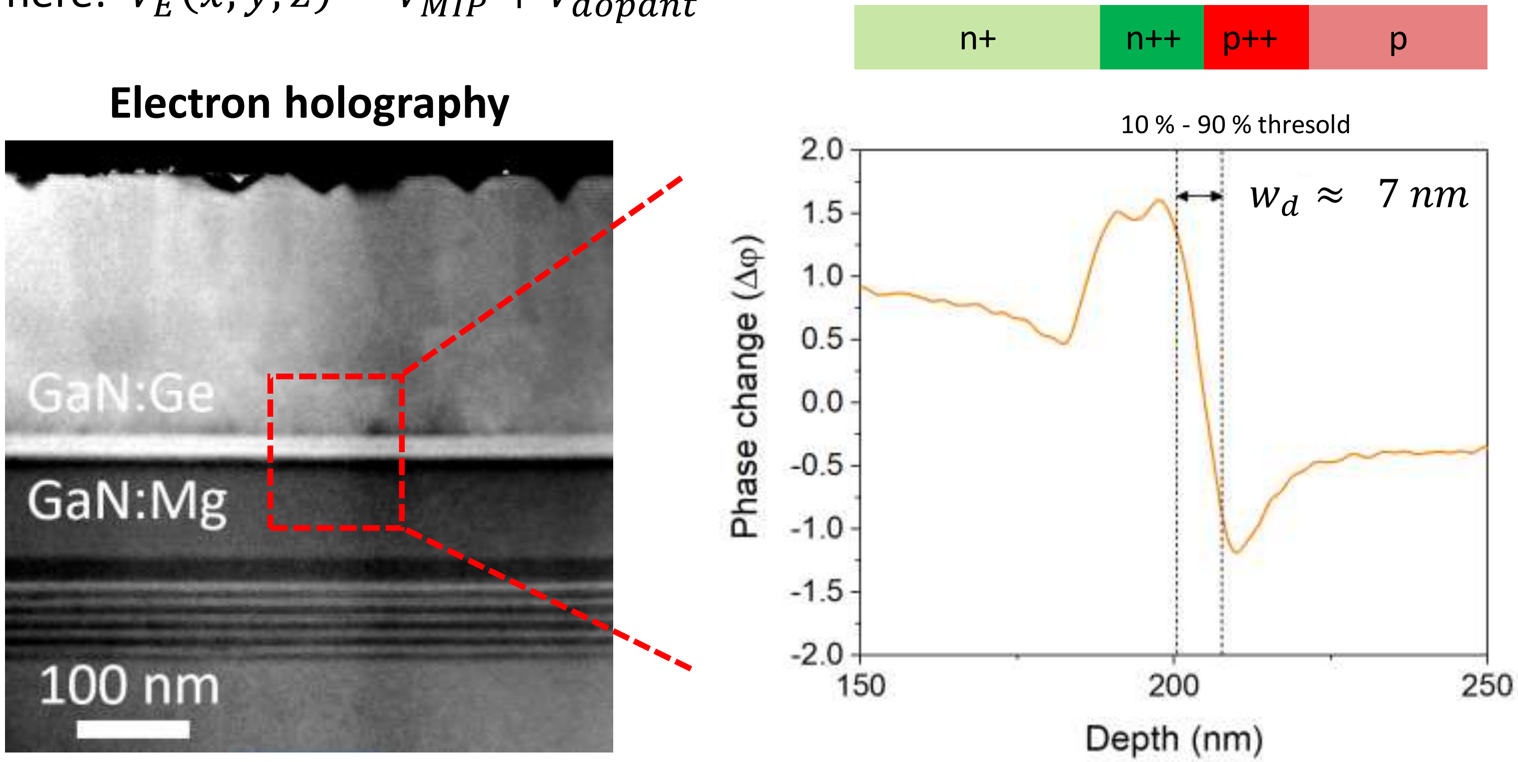

- High sensivity to active dopants spatial distribution.
- Holography is not quantitative in this case.

E. Di Russo, et al., Nanotechnology 31.46 (2020): 465706. *doi.org/10.1088/1361-6528/ab996c*

Si/Mg hybrid-tunnel junction

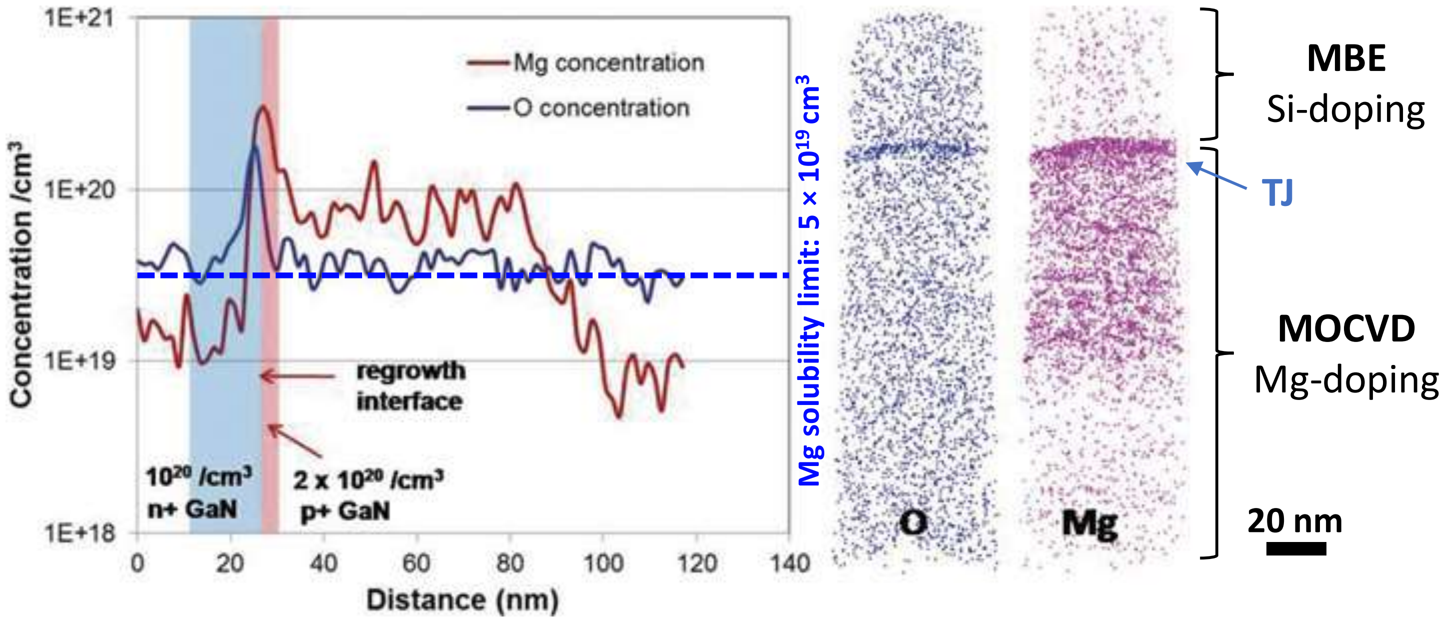

TJ fabrication process:

1) MOCVD p-GaN growth (**Mg-doping**);
2) atmosphere exposure and solvent cleaning;
3) MBE n-GaN regrowth (**Si-doping**).

❖ Residual surface **oxygen could enhance tunneling** as it is an electron donor in GaN: the regrowth interface acting as a thin δ-doped n-type layer in the middle of the TJ.

❖ δ-doped interface induces band bending in the p-GaN only, and effectively narrows the width of the depletion region. **The minimum tunneling distance *w* is reduced from 5.5 to 3.2 nm** at −0.5V for the δ-doped.

Band structure simulation

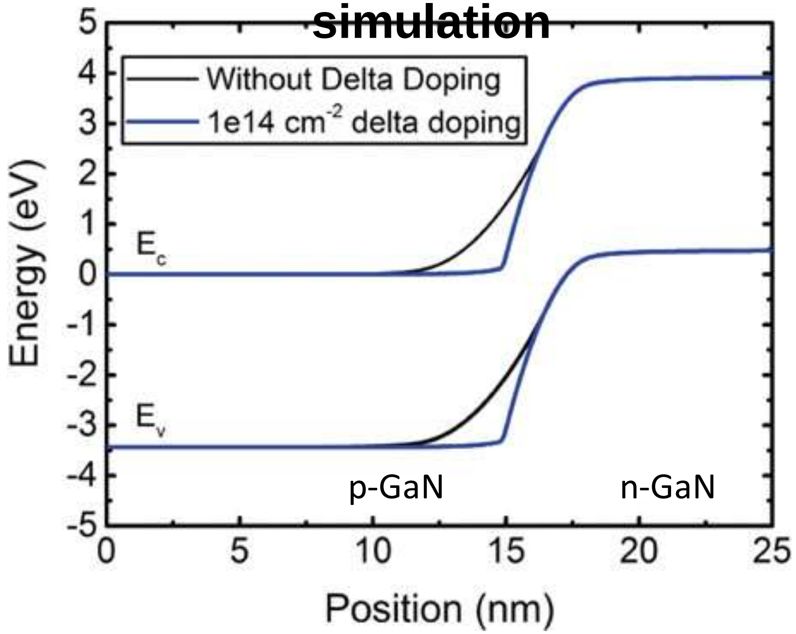

E. C. Young et al., Applied Physics Express 9.2 (2016): 022102. *doi.org/10.7567/APEX.9.022102*

Mg diffusion along dislocations

AS BeST

p-n diode

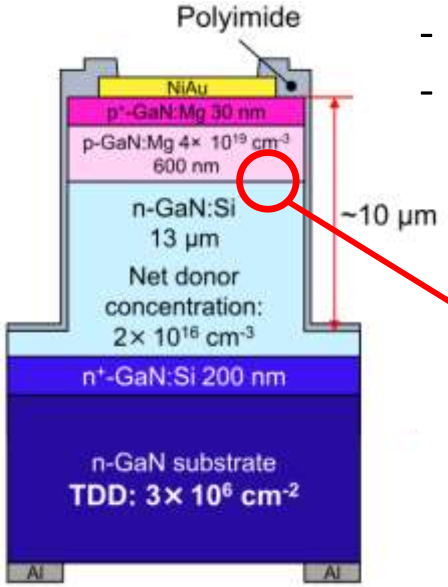

- Removal of p-type layer
- KOH etch pit formation

Pit (SEM)

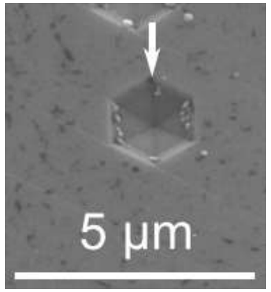

n-GaN:Si

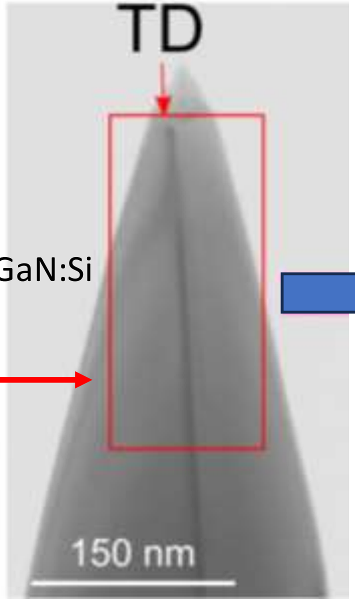

Iso-concentration surface with 0.4% at.% Mg

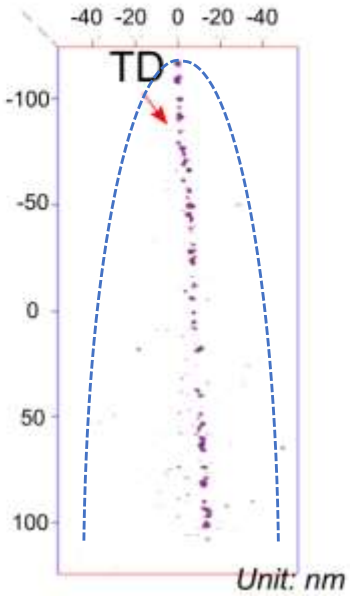

- Direct evidence of Mg "**pipe-diffusion**" through TDs has not yet been observed until 2019.

❖ **Mg from p-GaN diffused through the mixed dislocations.** Mg atoms concentrate in a 4 nm diameter region around dislocations. Theoretical studies suggest that the diffusivity of interstitial Mg at the dislocation core is three orders of magnitude larger than the outside region at 1000 K.

❖ Mg+dislocation complexes causes n-type behavior even in the p-type region, acting as current shunts and result in device failure.

S. Usami et al., Applied Physics Letters 114, 232105(2019). *doi.org/10.1063/1.5097767*

Part II

Hyper-doping in Si

B and Ga doping

B and Ga doping in Si

- **B**: sufficient solubility and diffusion rate that allows easy control of junction depths.
- **Ga**: promising for solar cells, due to its long minority carrier lifetime with no lifetime degradation.

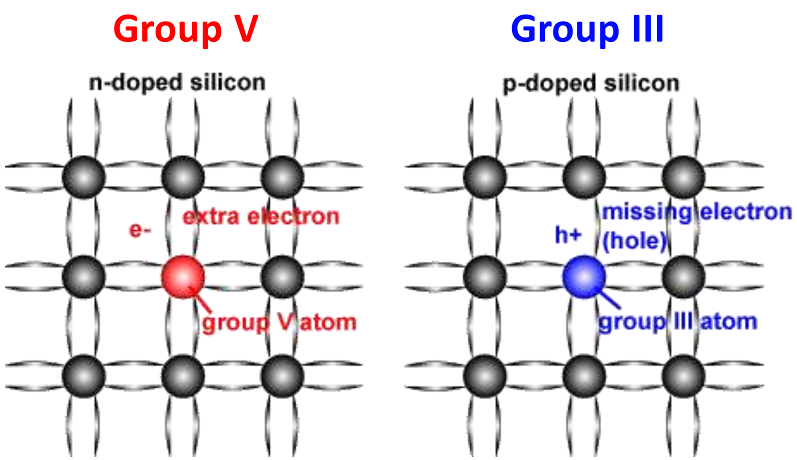

DOPANT ACTIVATION:
in **poly-Si** by flash-assisted rapid thermal annealing
(~1 ms, 1150-1350°C).

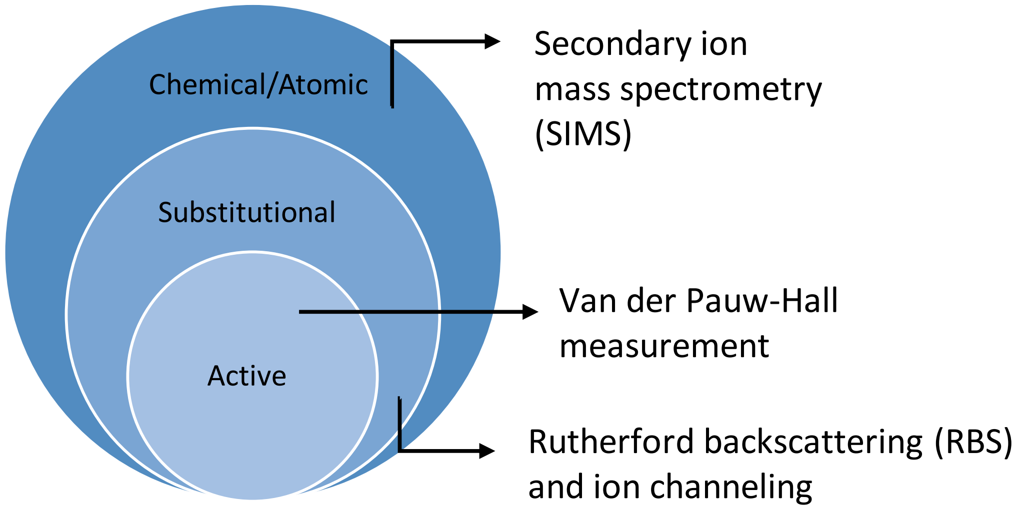

- Enhancement in B diffusivity in the **grain boundaries**

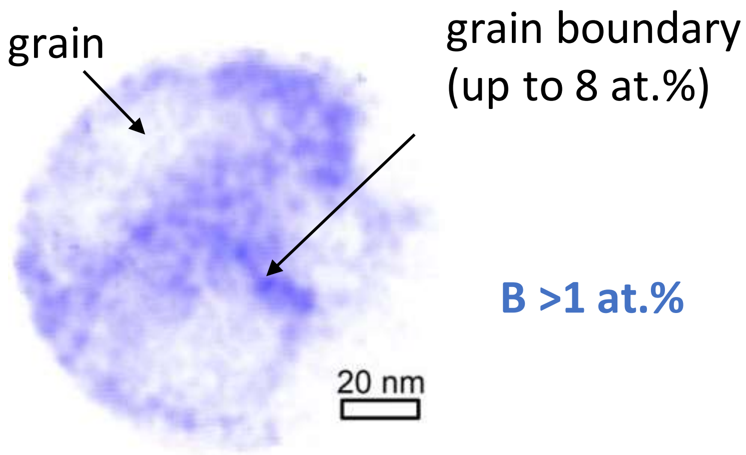

S. Jin et al., Journal of Applied Physics, vol. 111, no. 4, p. 044508, 2012. *doi.org/10.1063/1.3688246*

Pulsed laser melting

ns laser pulse

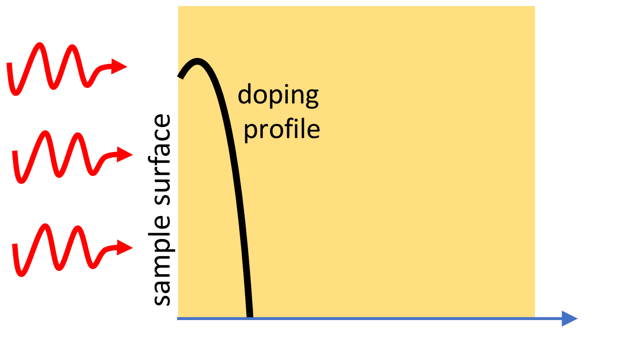

*also in air athmosphere

ADVANTAGES:

- Diffusion confined within the molten phase.
- Excellent final crystalline quality.
- Compatible with the CMOS backend-of-line (BEOL).
- Very high lateral control & large areas.
- Hyper-doping (v >1 m/s).

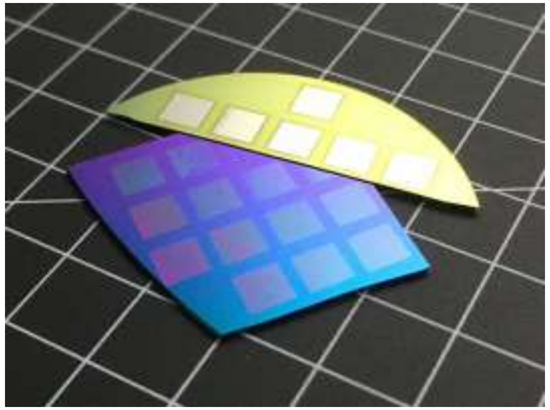

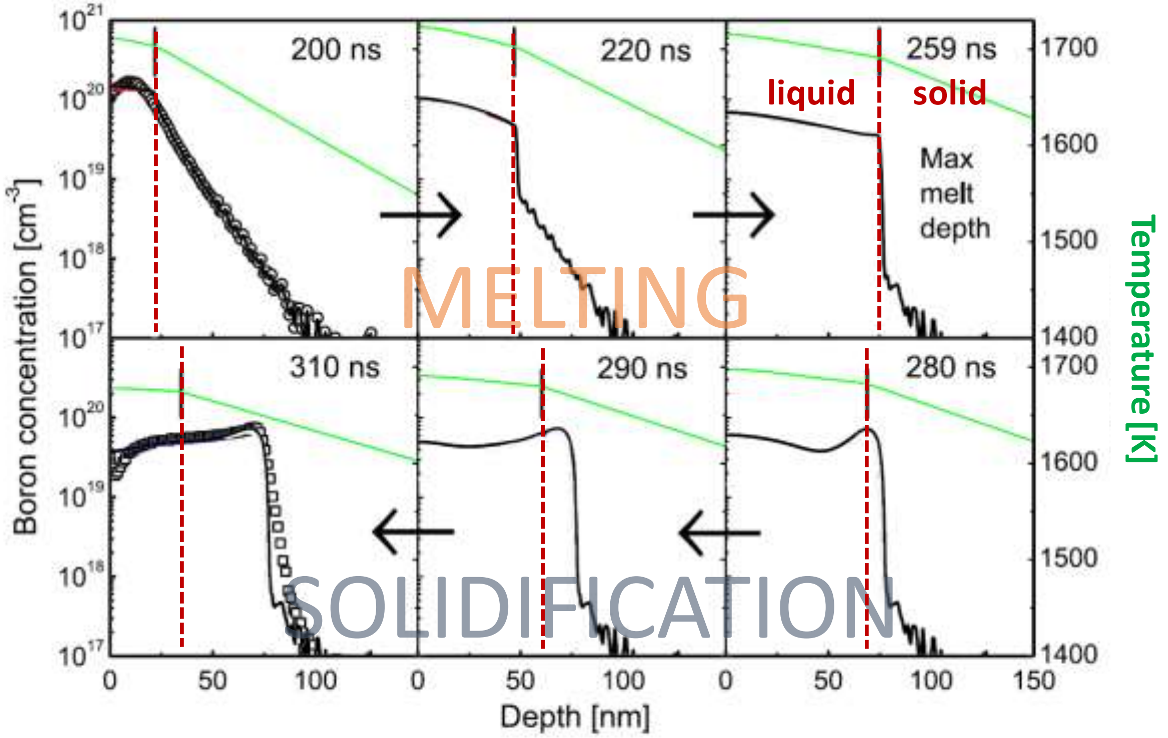

G. Fisicaro et al., Physical Review Letters 110.11 (2013): 117801. *doi.org/10.1103/PhysI*

B and Ga doping in Si

Chief Operator & former interface

Coherent COMPex laser
pulse duration: 22 ns
laser wavelength: 248 nm

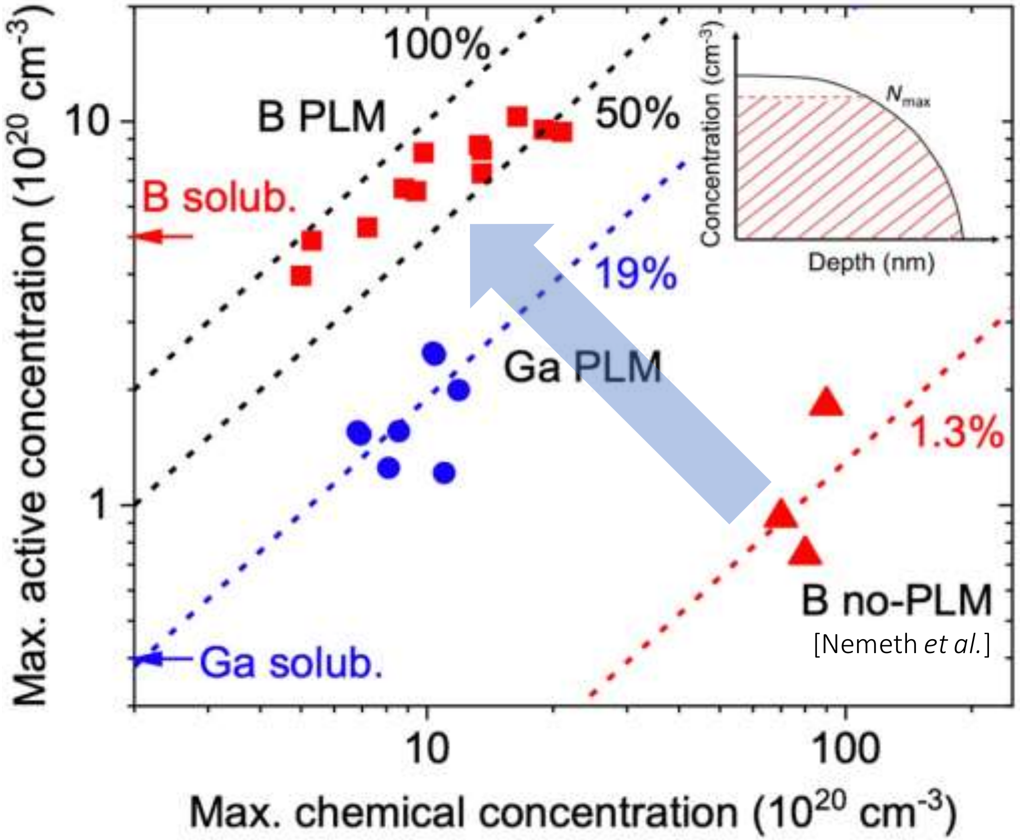

- Higher active doping concentration than solid solubility limits in Si after PLM, which was not possible by conventional furnace annealing.
- Pulsed laser melting is shown to successfully hyper-dope Si using both B and Ga.
- High degree of dopant activation: ~100% activation for B and ~20% for Ga.

K. Chen et al., Energy & Environmental Materials 6.3 (2023): e12542. *doi.org/10.1002/eem2.12542*

Part II

Hyper-doping in Ge

Sb doping

Pulsed laser melting

Ex-situ diffusion of dopants developed at the University of Padova

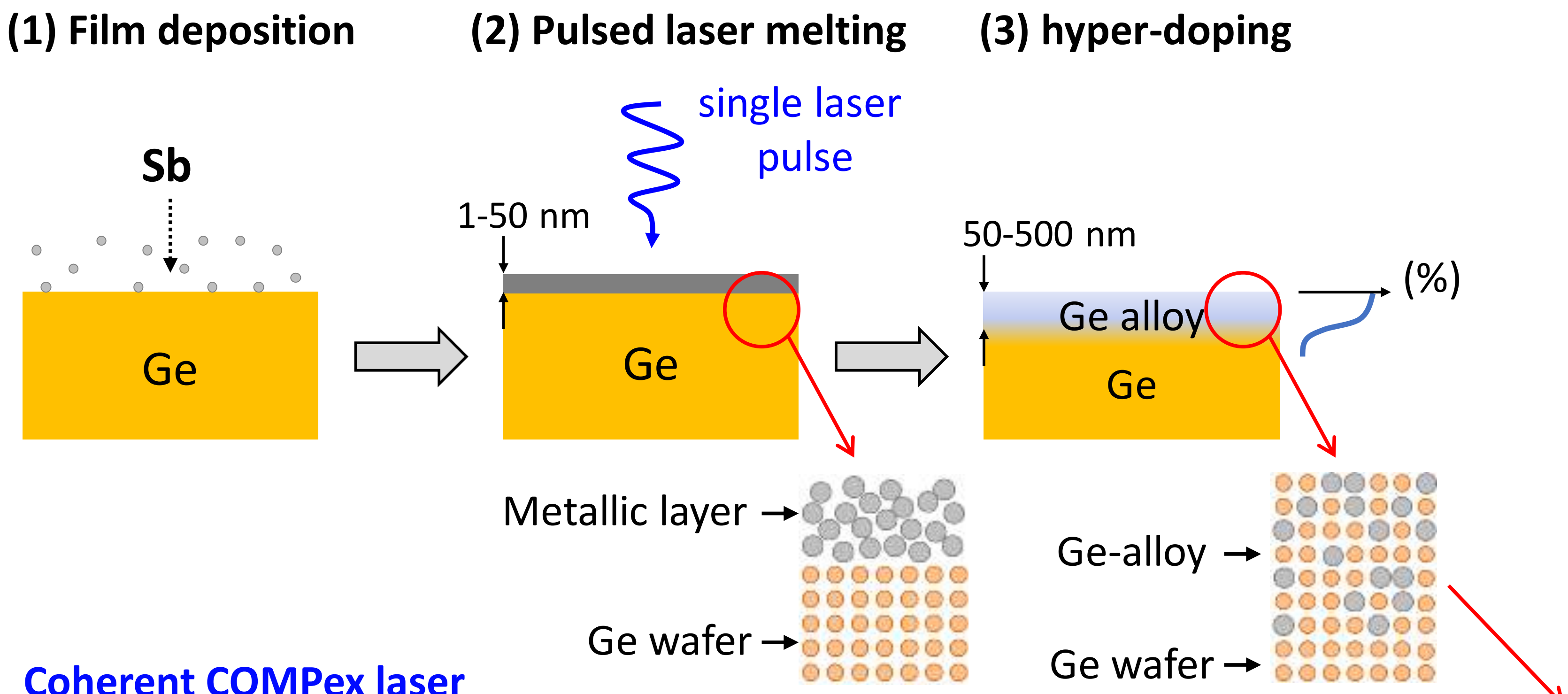

Coherent COMPex laser
pulse duration: 22 ns
laser wavelength: 248 nm

- **Very economic**:
  - deposition via sputtering or e-beam;
  - PLM performed in air.
- **Local alloying**: high spatial control obtained thanks to photolithography before deposition or laser shadow masks.
- High reproducibility and doping activation.

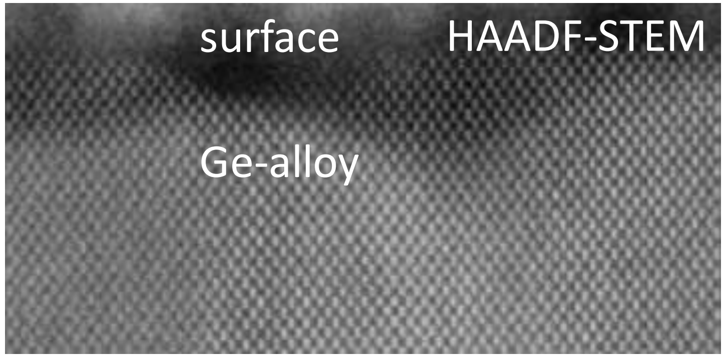

[1] E. Di Russo et al., Applied Surface Science 600 (2022): 154112. *doi.org/10.1016/j.apsusc.2022.154112.*

In diffusion of Sb doping in Ge

- Laser process parameters (i.e., pulse number, laser wavelength, …) have no major effects on the activation of the dopant.

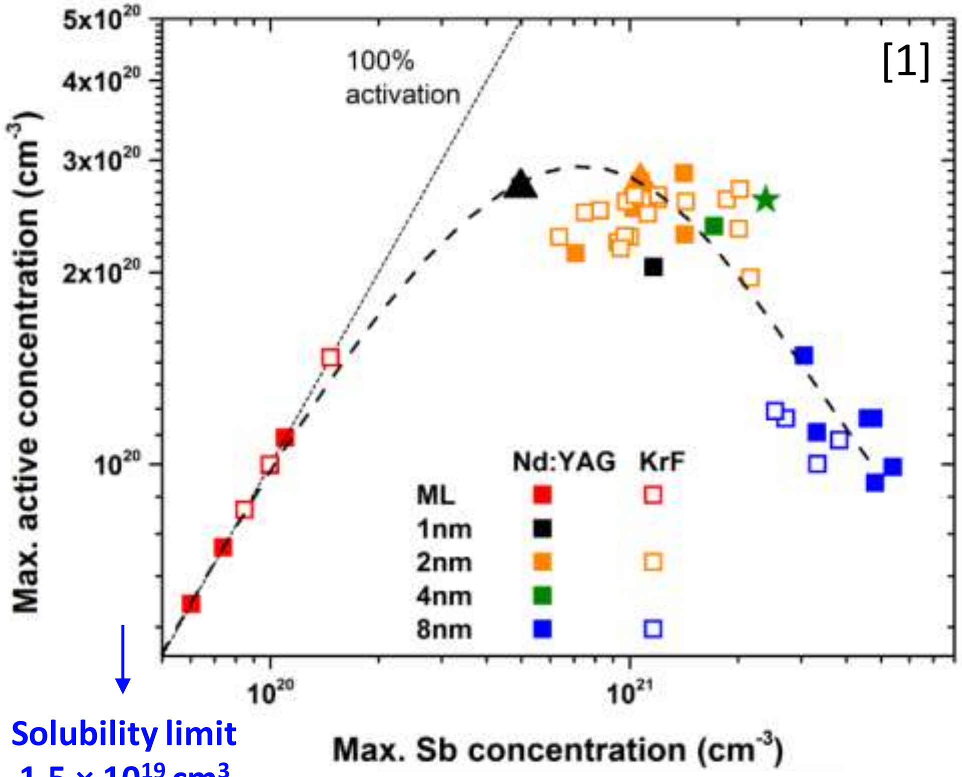

Solubility limit 1.5×10^{19} cm^3

Inactive dopant could be in the form of **small inactive Sb-V clusters**, where Sb atoms are just slightly displaced from the lattice sites.

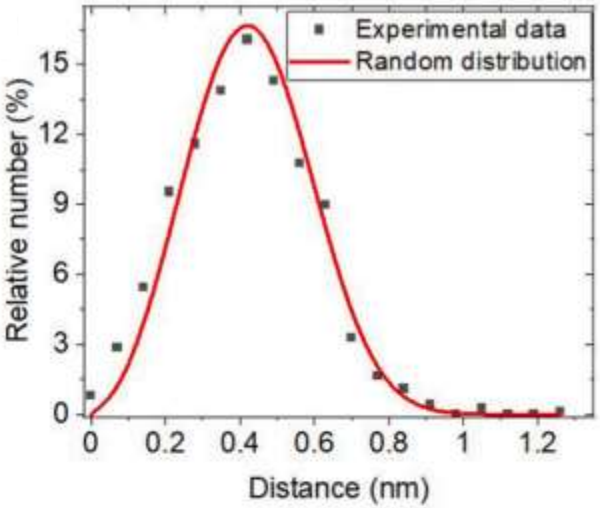

Sb atoms **segregate** in correspondence of defects.

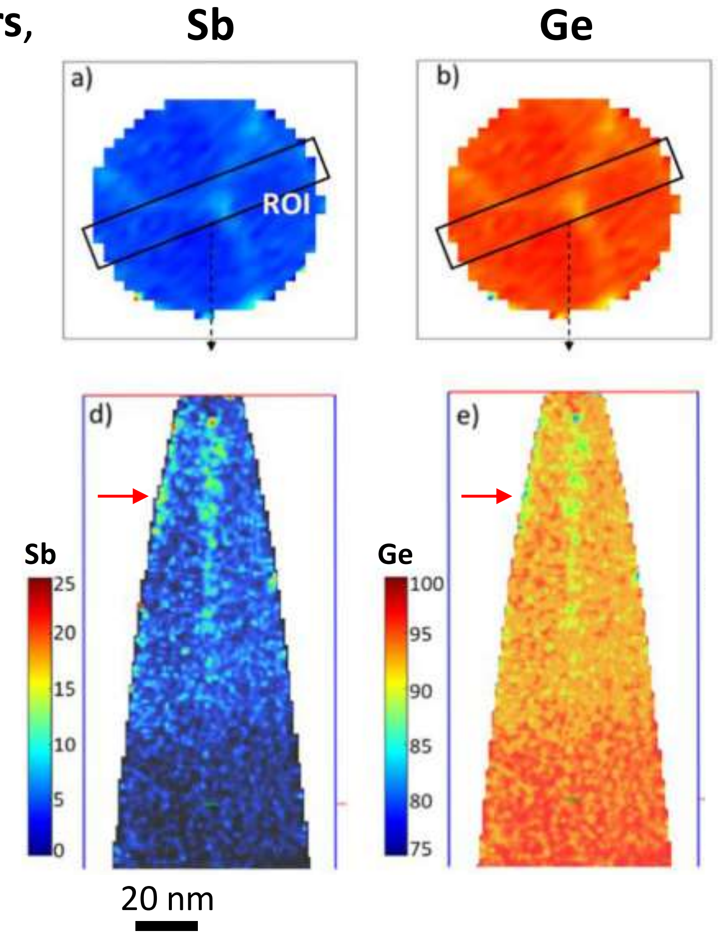

[1] C. Carraro et al., Applied Surface Science 509 (2020): 145229. *doi.org/10.1016/j.apsusc.2019.145229.*

[2] S. Ndiaye et al., Materials Science in Semiconductor Processing 164 (2023): 107641. *doi.org/10.1016/j.mssp.2023.107641.*

Pulsed laser melting

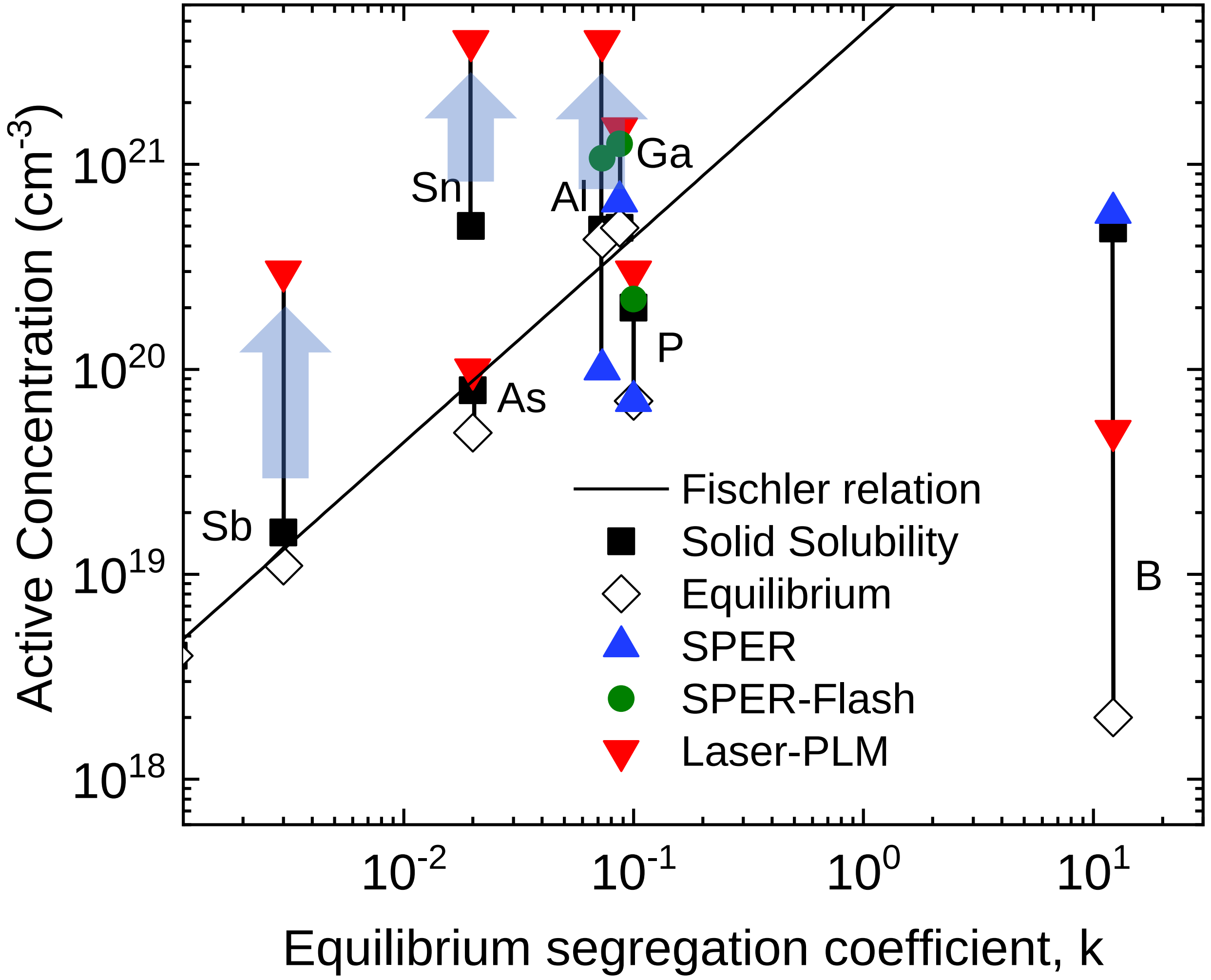

Doping in Ge at the University of Padova

- Segregation effects arise because we have mixed phases in equilibrium. A segregation coefficient can be defined to assess the magnitude of the effect.

$$k_{eff}(v) = \frac{v/v_D + k_{eq}}{v/v_D + 1}$$

$$\lim_{v \to \infty} k_{eff}(v) = 1$$

Conclusions

Main objectives of this lecture:

- Get familiar with the main techniques for investigating doping at the nanometric scale.
- Understand the link between chemical and active concentration in semiconductors.
- Achieve advanced knowledge concerning some doping segregation mechanism.

MAKE DOPING GREAT AGAIN!

Thank you for your attention!

Dipartimento di Fisica e Astronomia Galileo Galilei

Università degli Studi di Padova

ASBeST

Roma - 17/05/2024

Doping and Hyper-doping

Enrico Di Russo

BACKUP

Obsidian: silica (SiO_2) and sodium/potassium oxides

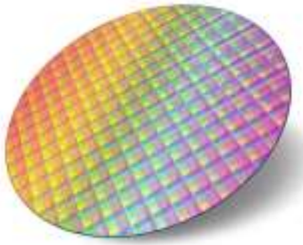

Transforming material *Transforming energy* *Transforming information*

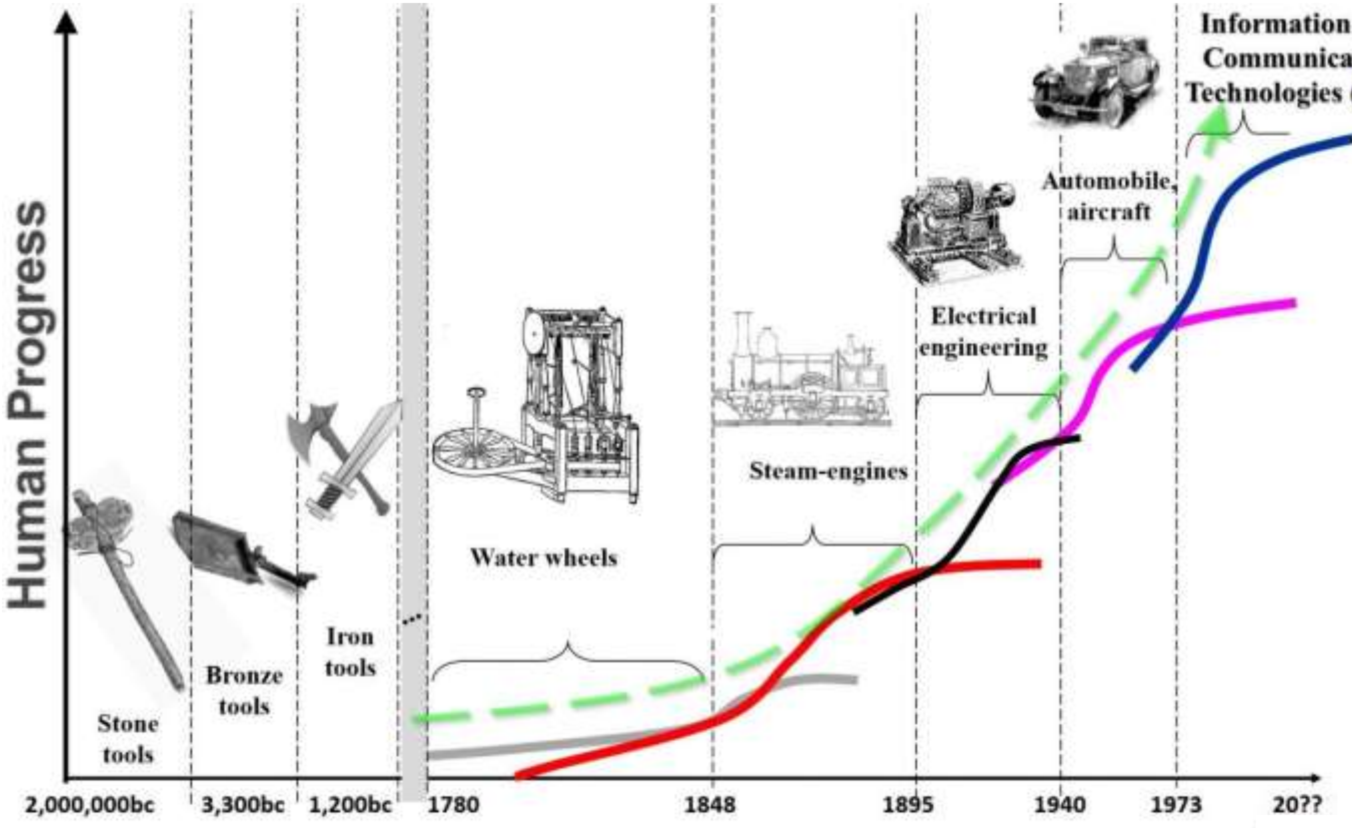

M. Hilbert, Online Course *Digital Technology & Social Change*, University of California: https://canvas.instructure.com/courses/949415

In 1931, Wolfgang Pauli said:

"One shouldn't work on semiconductors, that is a filthy mess; who knows whether any semiconductors exist".

GaN grown by metalorganics-chemical-vapour-deposition (MOCVD)

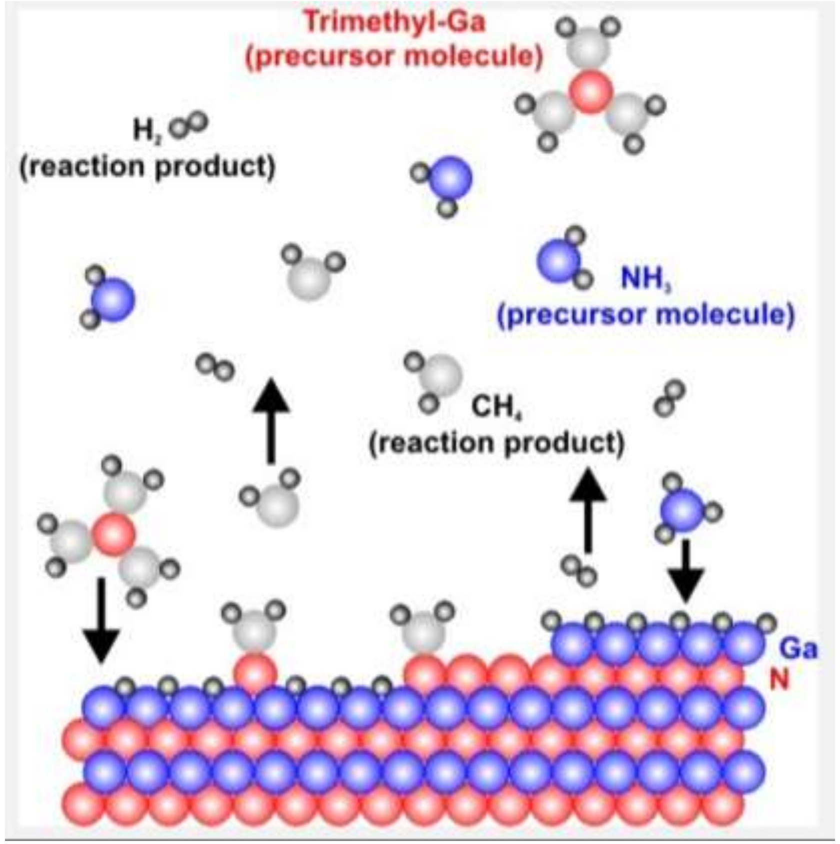

Growth temperature:
900-1000 °C

Carrier gas transports the MOCVD precursors (e.g., trimethyl gallium, ammonia) into the reactor, where they undergo pyrolysis or chemical reaction. Ga and N absorb onto the semiconductor wafer surface, resulting in their incorporation into the epitaxial structure of the semiconductor crystal lattice.

ADVANTAGES:
- Faster growth rate than molecular beam epitaxy (MBE);
- No UHV needed (compared to MBE);
- High temperature growth (process thermodynamically favourable);
- Cheap methodology.

DISAVANTAGES:
- Human hazard (corrosive and toxic gasses);
- Carbon contamination and H incorporation are sometimes a problem.

Molecular beam epitaxy (MBE)

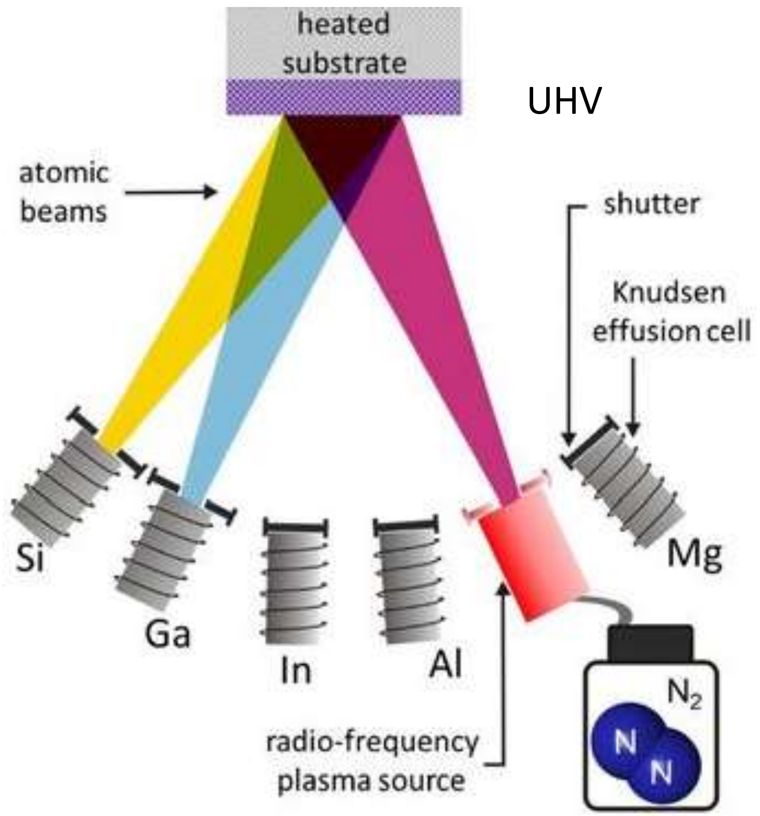

MBE is based on the **effusion evaporator source** (Knudsen Cell) principle, which states that evaporated from a hot surface into a low-pressure gas phase travel through a vacuum towards a substrate where they condense into a thin film.

ADVANTAGES:

- High purity growth;
- Hydrogen free environment;
- Possibility to use plasma or laser assisted growth

DISAVANTAGES:

- Need ultra-high vacuum;
- Low growth rate;
- Very expensive.

Transmission Electron Microscopy (TEM): Electron Holography

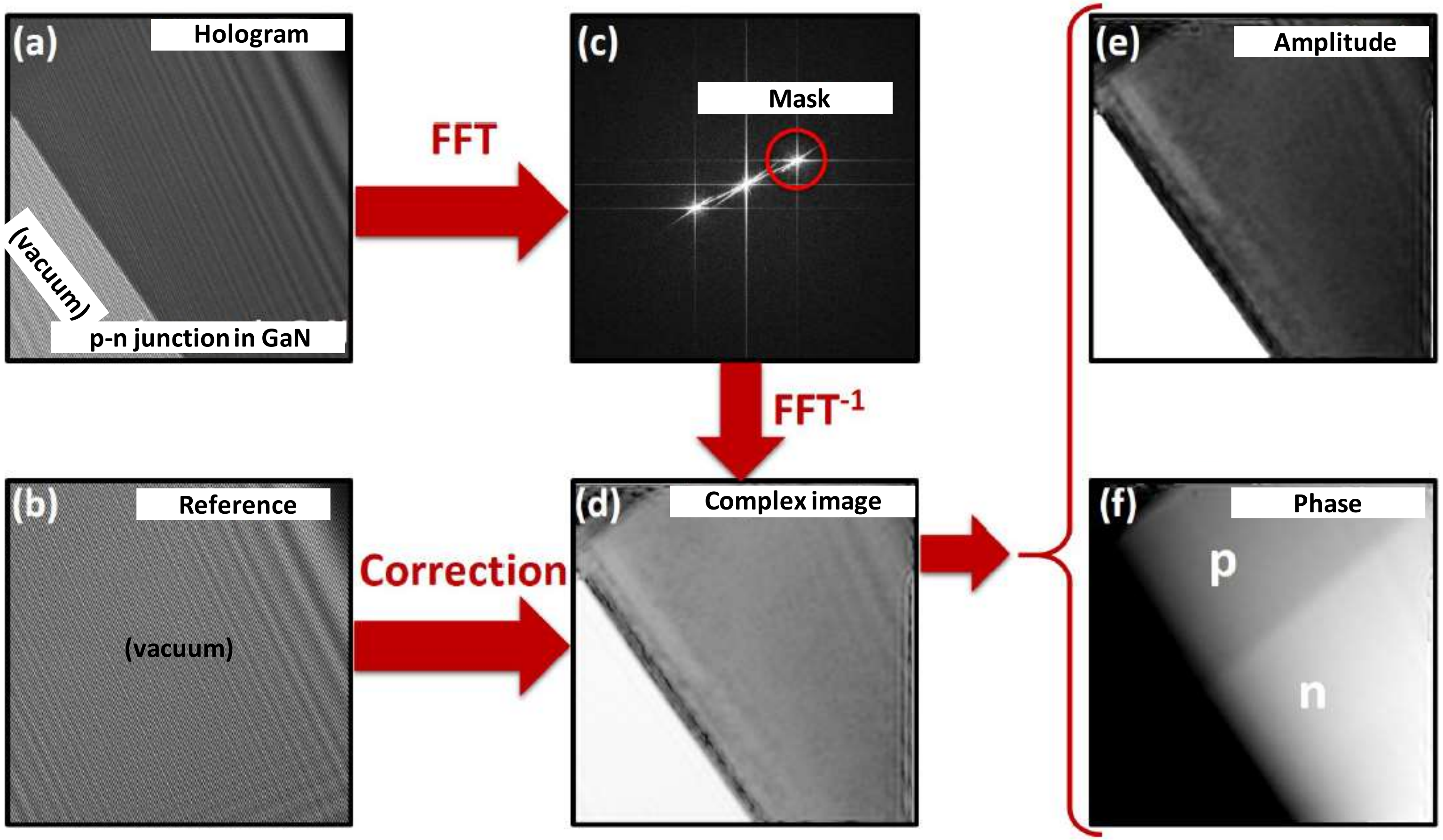

Phase: $$\phi_e = \phi_{dopant} + \phi_{MIP} = C_E \int_0^t V_{dopant}(r,z)dz + C_E \int_0^t V_0(r,z)d(z)$$

B and Ga doping in Si

Segregation of B dopants to grain boundaries in poly-Si after flash-assisted rapid thermal annealing (1150-1350 °C) is observed by APT.

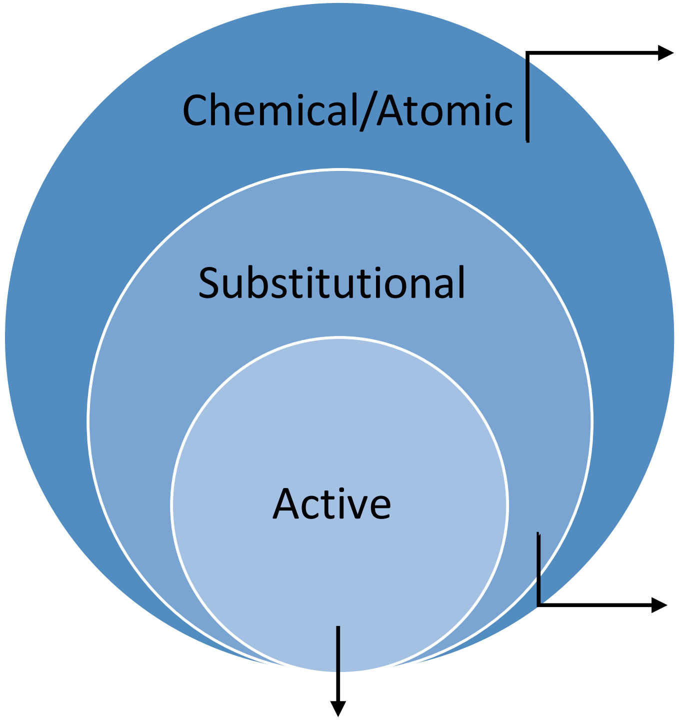

Secondary ion mass spectrometry (SIMS)

Rutherford backscattering (RBS) and ion channeling

Van der Pauw-Hall measurement

Inter-grain

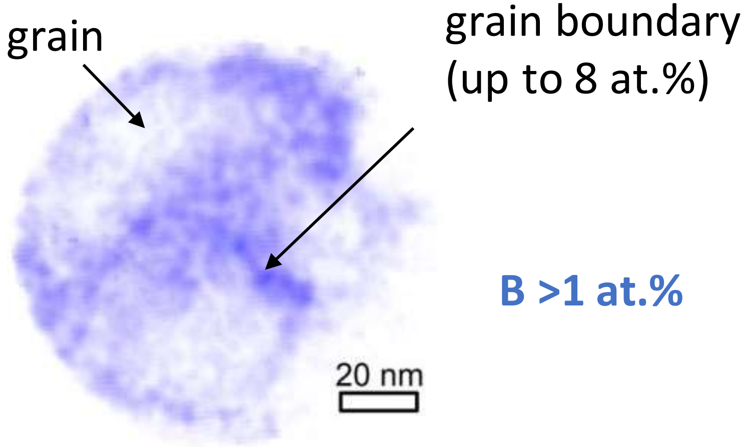

B >1 at.%

Intra-grain

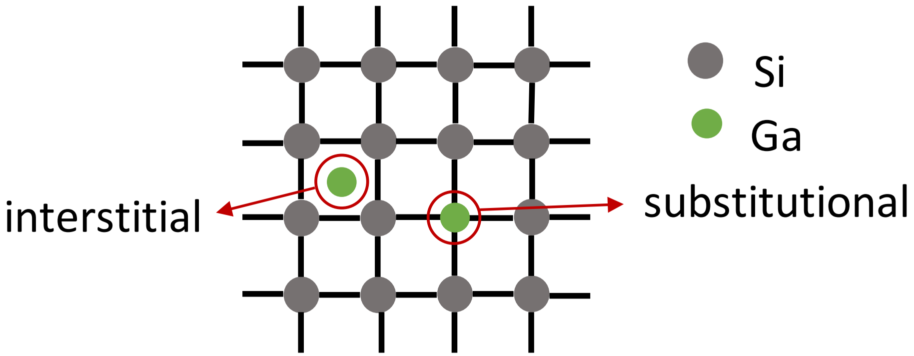

S. Jin et al., Journal of Applied Physics, vol. 111, no. 4, p. 044508, 2012. *doi.org/10.1063/1.3688246*